nclassified

curity Classification of this page

REPORT DOCUMENTATION PAGE

1a Report Security Classification: Unclassified		1b Restrictive Markings	
2a Security Classification Authority		3 Distribution/Availability of Report Approved for public release; distribution is unlimited	
2b Declassification/Downgrading Schedule			
4 Performing Organization Report Number(s)		5 Monitoring Organization Report Number(s)	
6a Name of Performing Organization Naval Postgraduate School	6b Office Symbol *(if applicable)* 31	7a Name of Monitoring Organization Naval Postgraduate School	
6c Address *(city, state, and ZIP code)* Monterey CA 93943-5000		7b Address *(city, state, and ZIP code)* Monterey CA 93943-5000	
8a Name of Funding/Sponsoring Organization	6b Office Symbol *(if applicable)*	9 Procurement Instrument Identification Number	
8c Address *(city, state, and ZIP code)*		10 Source of Funding Numbers	
		Program Element No	Project No / Task No / Work Unit Accession No

11 Title *(include security classification)*
Lift Enhancement of a Wing/Strake Using Pneumatic Blowing

12 Personal Author(s) Zgraggen, Craig J.

13a Type of Report	13b Time Covered From To	14 Date of Report *(year, month, day)*	15 Page Count 92
Master's Thesis		March 1993	

16 Supplementary Notation The views expressed in this thesis are those of the author and do not reflect the official policy or position of the Department of Defense or the U.S. Government.

17 Cosati Codes			18 Subject Terms *(continue on reverse if necessary and identify by block number)*
Field	Group	Subgroup	Strake, Vortex Control, Blowing, Vortex Interaction, Pneumatic, Enhanced Lift

19 Abstract *(continue on reverse if necessary and identify by block number)* A low-speed wind-tunnel study to quantitatively measure the lift and drag effects of pneumatically controlling strake and leading-edge vortices generated by a half-span, generic-fighter model was conducted. The study measured the increase in lift and drag on the model throughout a range of angles of attack. The study utilized various blowing tubes of different geometries and orientations. Results showed that blowing produced changes in lift with minimal effect on drag. Blowing appeared to reattach flow during the initial stages of stall. Blowing increased lift a maximum of 9 percent at an angle of attack of 20 degrees, and up to 7 percent at angles of attack greater than 20 degrees. Blowing rates were varied from a C_μ of 0.0094 to a C_μ of 0.022. Near axial blowing produced the largest increases in lift. It was found that lift increases were directly proportional to changes in blowing rate.

20 Distribution/Availability of Abstract	21 Abstract Security Classification	
Unclassified/unlimited x same as report __ DTIC users	Unclassified	
22a Name of Responsible Individual Richard M. Howard	22b Telephone *(include Area Code)* 408 656 2870	22c Office Symbol AA/Ho

DD FORM 1473,84 MAR 83 APR edition may be used until exhausted security classification of this page

All other editions are obsolete Unclassified

T259333

Approved for public release; distribution is unlimited

LIFT ENHANCEMENT OF A WING/STRAKE USING PNEUMATIC BLOWING

by

CRAIG J. ZGRAGGEN
Lieutenant, United States Navy
B.S., Gannon University, 1984

Submitted in partial fulfillment
of the requirements for the degree of

MASTER OF SCIENCE IN AERONAUTICAL ENGINEERING

from the

NAVAL POSTGRADUATE SCHOOL
March, 1993

ABSTRACT

A low-speed wind-tunnel study to quantitatively measure the lift and drag effects of pneumatically controlling strake and leading-edge vortices generated by a half-span, generic-fighter model was conducted. The study measured the increase in lift and drag on the model throughout a range of angles of attack. The study utilized various blowing tubes of different geometries and orientations. Results showed that blowing produced changes in lift with minimal effect on drag. Blowing appeared to reattach flow during the initial stages of stall. Blowing increased lift a maximum of 9 percent at an angle of attack of 20 degrees, and up to 7 percent at angles of attack greater than 20 degrees. Blowing rates were varied from C_μ of 0.0094 to C_μ of 0.022. Near axial blowing produced the largest increases in lift. It was found that lift increases were directly proportional to changes in blowing rate.

TABLE OF CONTENTS

Page

Abstract.....iii

Table of Contents.....iv

I. Introduction.....1

II. Background.....4

A. Forebody Blowing.....4

1. Lemay, Sewall, and Henderson.....4

2. Guyton and Maerki.....6

3. Cornelius, Pandit, Osborn, and Guyton.....8

B. Combination Blowing.....9

C. Wing/Strake Blowing.....10

1. Miller and Gile.....10

2. Lemay and Rogers.....11

3. Roach and Kuhlman.....13

4. Willson and Howard.....15

D. Kern's Wing/Strake Junction Study.....16

III. Experiment and Procedure.....19

A. Overview.....19

B. Apparatus.....19

1. Wind Tunnel.....19

2. Wing/Strake Model.....22

3. Mass Flowmeter and Blowing Apparatus.....22

4. Balance and Turntable.....26

5. Data Acquisition Hardware.....26
6. Data Acquisition Software.....27
C. Experimental Conditions.....28
D. Experimental Procedure.....30
1. Pre-run Calibration and Test.....30
2. Testing Procedures.....32
3. Tests Holding C_μ Constant, Varying AOA.....34
4. Tests Holding AOA Constant, Varying C_μ.....36
5. Tests Varying Tube Inclination Angle.....37
E. Experimental Corrections.....38
IV. Discussion and Results.....40
A. Overview.....40
B. Baseline Model Performance.....40
C. Tests Holding C_μ Constant Varying AOA.....43
1. Blowing Port 1.....43
2. Blowing Port 2.....47
D. Tests Holding AOA Constant, Varying C_μ.....49
E. Tests Varying Tube Inclination Angle.....52
V. Conclusions and Recommendations.....55
A. Conclusions.....55
B. Recommendations.....56
List of References.....58
Appendix A. Balance Calibration.....60
Appendix B. Model Design.....68
Appendix C. Additional Figures.....75

Appendix D. Data Acquisition Program.....77

INITIAL DISTRIBUTION LIST.....85

I. INTRODUCTION

The modern tactical fighter is a technological wonder, with fly-by-wire controls and look-down shoot-down weapon systems. However, no matter how advanced the armament system, the pilot must still maneuver his aircraft into the release envelope before his opponent does. In a dog fight the more maneuverable aircraft has the advantage, and will most likely win the encounter.

One method by which current-generation fighters have been able to exploit the high-angle-of-attack (AOA > 20 degrees) regime is through the use of strakes. The strake produces a strong vortex which extends over the wing to enhance aircraft performance.

The ability to control the aircraft diminishes as the angle of attack (AOA) increases. The vortex bursts, allowing the vertical tail to be engulfed in the separated flow of the wing and to loose the ability to generate yawing moments. This loss of yaw moment can result in the reduction of available roll rate about the velocity vector. Also, vortex bursting creates an unsteady flow which can cause large transient loads on the vertical tail, leading to fatigue and premature structural failure, such as with the F/A-18 aircraft. The vortex of the strake also intertwines with the wing vortex and forebody vortex, producing an effect

detrimental to the production of lift. All of the results of vortex bursting at high angles of attack can eventually lead to a departure from controlled flight and possible loss of the fight and the aircraft.

There recently have been many research investigations into methods of controlling both the strengths and positions of the wing, strake, and forebody vortices. The research has concentrated on controlling the vortices by use of pneumatic blowing on either the forebody or the wing/strake surface. These studies have shown that blowing increases the strength of the vortices and delays burst location. Blowing results in indications of increases in lift, or an increase in yaw and roll moments through asymmetric blowing. The position of the vortices are also controllable, allowing a reduction of the intertwining of the vortices and delaying vortex breakdown. The majority of the studies have concentrated on flow visualization of the vortices. Little research has been done to obtain quantitative measurements of the amount of lift enhancement due to blowing. [Ref.1-8]

The purpose of this research was to obtain quantitative measurements of lift enhancement due to pneumatic blowing on a wing/strake configuration. Comparisons were made regarding blowing port position, blowing coefficient, blowing angle, and blowing tube inclination angle. A half-span wooden model with a generic planform, similar in size and shape to the F/A-18 aircraft, with a strake similar to that of the YF-23, was used

for data collection. This comparison focused on the amount of additional lift generated by controlling the strake and wing vortices with pneumatic blowing.

II. BACKGROUND

Vortex breakdown behavior has been studied for slightly over a decade. The past three years have seen an increase in research into vortex control through pneumatic blowing. The research has focused in two areas: controlling the forebody vortex with forebody blowing; controlling the strake vortex with wing/strake blowing. The data have been collected through flow visualization (velocity profile mapping) and quantitative force measurements.

A. FOREBODY BLOWING

1. Lemay, Sewall, and Henderson

Lemay, Sewall, and Henderson [Ref. 1] conducted a wind-tunnel test which studied the effects of tangential slot and jet-nozzle forebody blowing on a 1/15 scale model F-16C. A freestream Mach number of 0.4 and Reynolds number of 2.5 million per foot were the test conditions. Two jet-nozzle locations and one tangential slot-nozzle location were investigated (Figure 1, [Ref. 1]). Blowing coefficients (C_μ) used ranged between 0.0016 and 0.0820.

C_μ was defined as:

$$C_\mu = \frac{\dot{m}_j V_j}{q_\infty S_{ref}} \qquad (1)$$

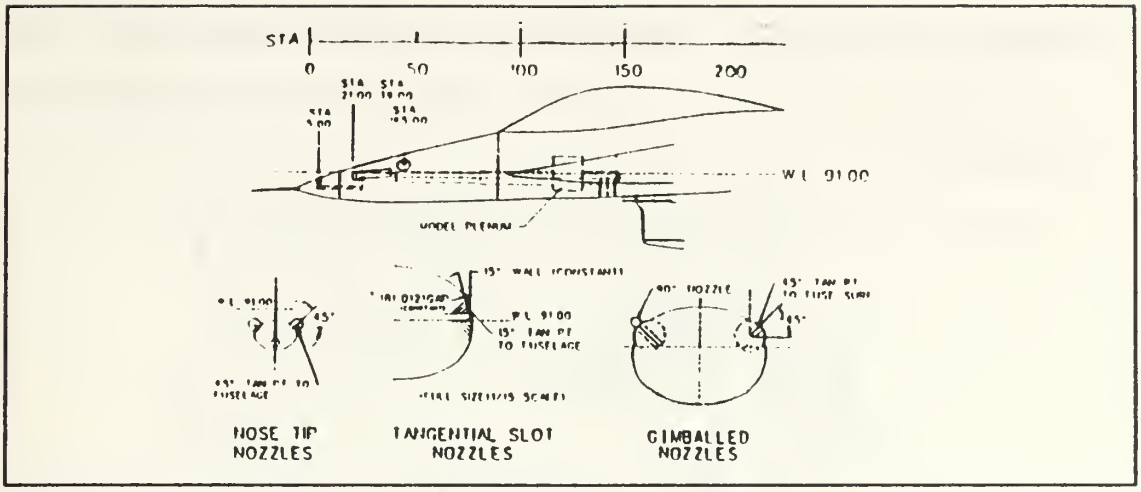

Figure 1. F-16C Forebody Model, [Ref. 1]

Where:

$\dot{m}_j$ mass-flow rate of the blowing jet

V_j sonic velocity of the blowing jet

q_∞ freestream dynamic pressure

S_{ref} model wing reference area

The results of the study showed an increase in yawing moments with blowing over all angles of attack, 0 degrees to 52 degrees, and sideslip, -20 degrees to 20 degrees (Figure 2a, 2b [Ref. 1]). The tangential slot forebody blowing was most effective at the lowest blowing coefficient tested, C_μ of 0.0016. The nose-tip jet nozzle was most effective at the highest blowing coefficient tested, C_μ of 0.0082. The results also showed that tangential slot blowing on the right side produced a nose-right yawing moment while blowing from the right-side nose tip-jet nozzle produced a nose-left yawing moment. The authors pointed out that nose-left yawing was opposite to other research results; however no specific

research was cited. A possible cause given was the different jet-nozzle locations used for this study and the previous research.

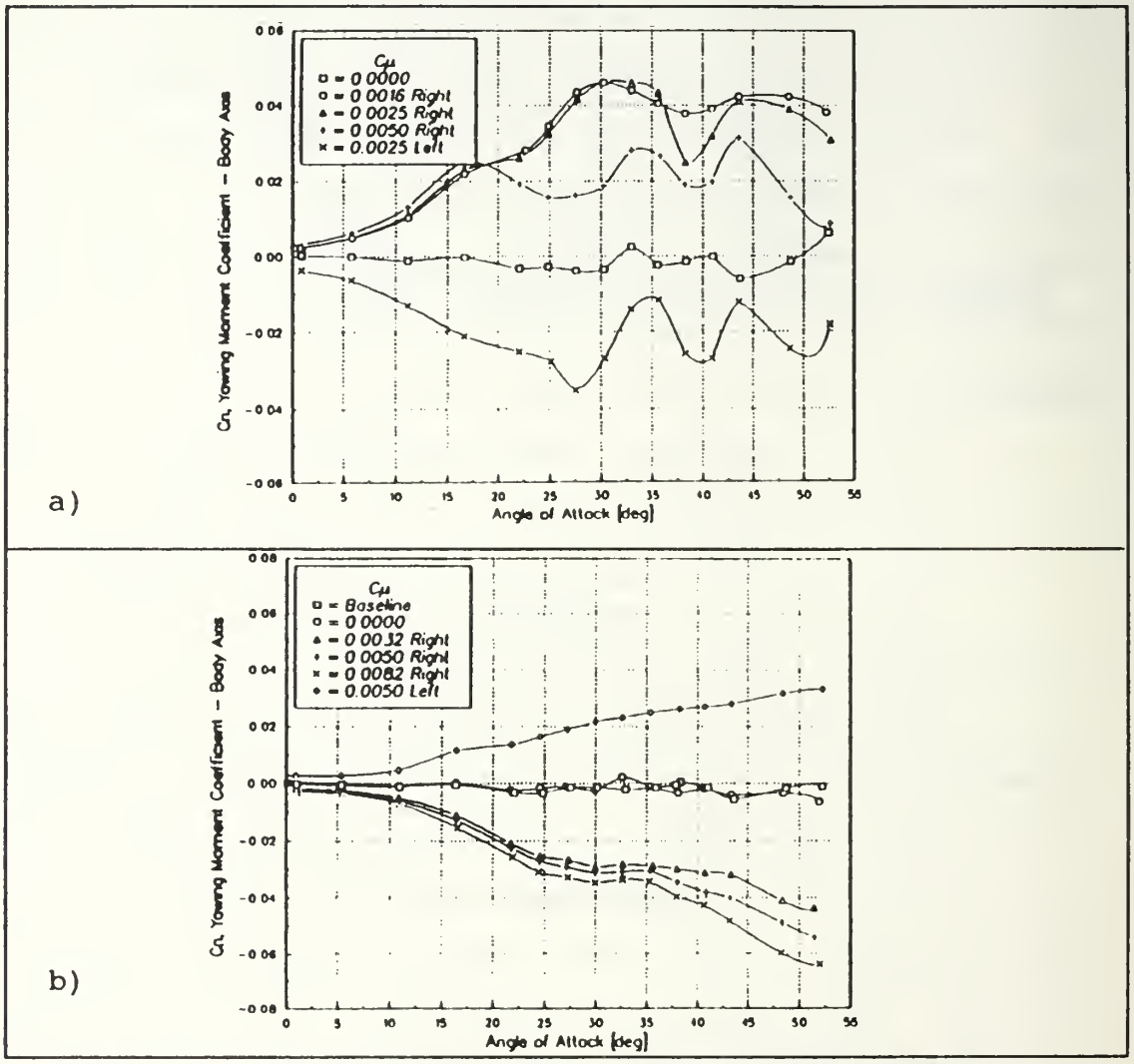

Figure 2. a) Tangential Slot C_n vs AOA, ß=0° [Ref. 1]
b) Jet Nozzle C_n vs AOA, ß=0° [Ref. 1]

2. Guyton and Maerki

Guyton and Maerki [Ref. 2] studied forebody vortex control on a 1/8-scale X-29 model. A single set of jet nozzles located 0.5 fuselage diameters back from the nose apex was used (Figure 3 [Ref. 2]). The tests were conducted in two

sets: the first with a complete scale model and the second with the isolated forebody.

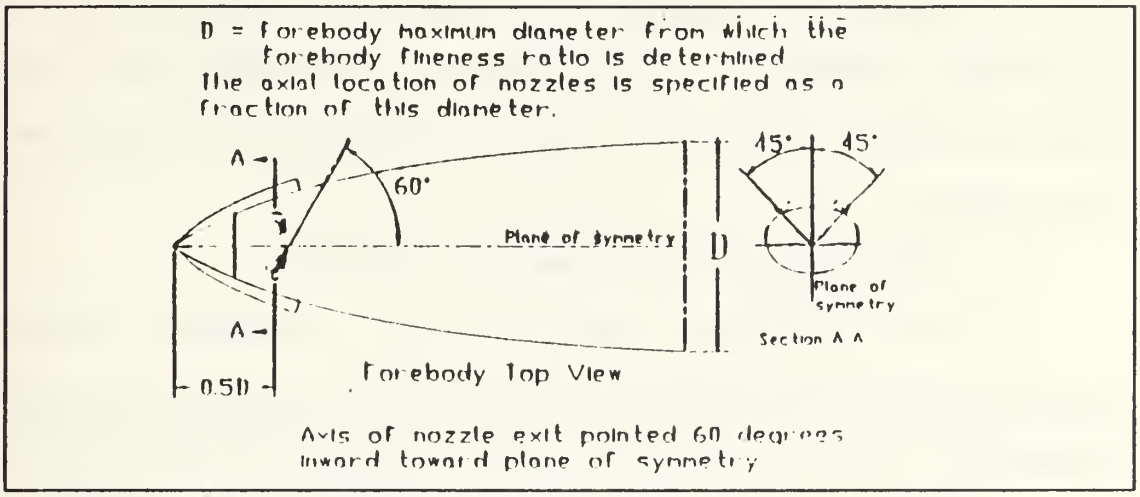
D = Forebody maximum diameter from which the forebody fineness ratio is determined
The axial location of nozzles is specified as a fraction of this diameter.
A
60°
Plane of Symmetry
D
A
0.5D
Forebody Top View
45°
45°
Plane of symmetry
Section A A
Axis of nozzle exit pointed 60 degrees inward toward plane of symmetry

Figure 3. X-29 Forebody Model, [Ref. 2]

The first test used the complete model. The angle of attack (AOA) varied from -4 to 44 degrees, and sideslip angle varied from -10 to 5 degrees. Blowing coefficients between 0.0 and 0.020 were used. The data showed a slight increase in right yawing moment with right-side blowing above 25 degrees AOA and strong yawing moment increase above 40 degrees AOA. The data indicated that in sideslip the effectiveness of the blowing disappeared as the model was yawed beyond ±5 degrees due to the downwind jet affecting the opposite-side vortex vice the jet-side vortex.

The second tests were conducted on the isolated-forebody model to compare with results in the full-model tests. The data indicated that blowing with a full model generated greater yawing moments than the isolated forebody as the blowing coefficient was increased. The increase was

possibly due to factors such as canard influence and forebody model reduced fineness.

The research showed that Mach number had little effect on yawing moments for blowing rates less than C_μ of 0.009, while it caused degradation with blowing coefficients above that value.

3. Cornelius, Pandit, Osborn, and Guyton

In another study using the X-29, Cornelius, Pandit, Osborn, and Guyton [Ref. 3] investigated a variety of nozzle geometries. Two nozzle blocks were mounted internally to the model, symmetrically about the centerline (Figure 4 [Ref. 3]). A strake was also mounted from the nose apex and extended to approximately 18 percent of the forebody-model length. Nozzles of different configurations were then placed at the forward blowing location. The most effective nozzle was found to be a slotted nozzle. The design was then modified with a smaller throat diameter. The smaller diameter nozzle showed improved results over the larger diameter nozzle at the same blowing coefficient.

The improved nozzle caused the jet to expand supersonically into a 2-D sheet to create a favorable interaction between the jet and flowfield. Investigation into nozzle orientation found a maximum yawing moment with the nozzle canted in 60 degrees from the longitudinal axis.

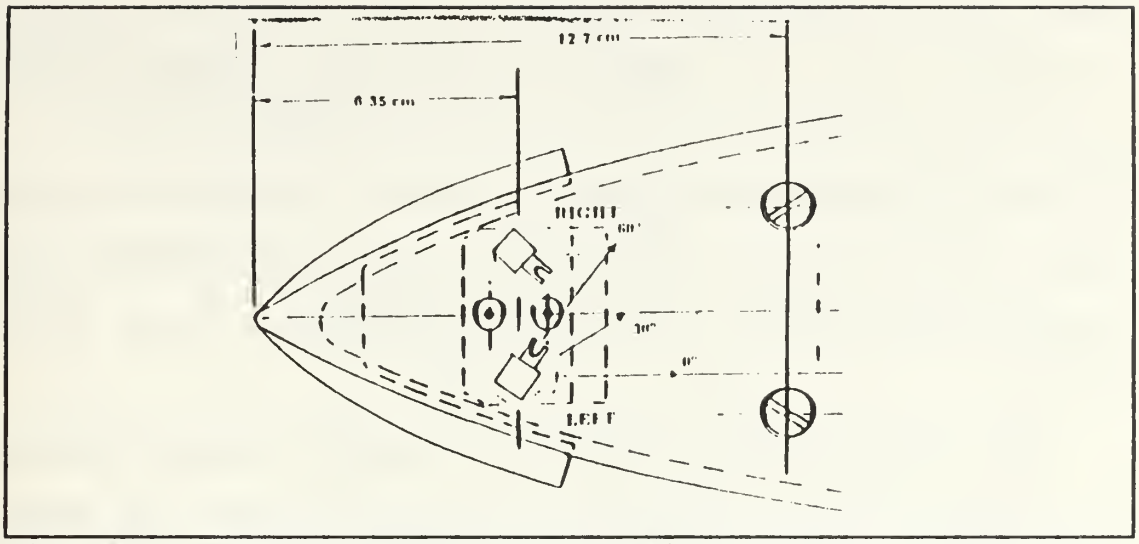

Figure 4. Forebody Model with Blowing Locations [Ref. 3]

B. COMBINATION BLOWING

Research conducted by Celik and Roberts [Ref. 4] investigated the effects of forebody-slot blowing and wing-slot blowing. They used a combination of a delta wing and a forebody with a cylindrical pointed ogive nose. The blowing slots on the wings were on the leading edges, while the forebody slots were along the cylindrical sides and not the ogive nose. Blowing through slots along the wings is not a common method used as a means of control. This investigation measured side forces, yawing moments, and rolling moments as a function of blowing coefficient.

The research showed a reversal of rolling moments with the application of mild (C_μ < 0.01) forebody blowing. This reversal was caused by a suction pressure peak at the blowing slot. As the blowing was increased, the vortex from the forebody moved toward the unblown side. This movement increased the strength of the forebody vortex on the unblown

side, and caused greater suction on the unblown side than on the blown side. It was also shown that forebody blowing produced a rolling moment four times greater than with the tangential wing blowing. Also, the model with rounded leading edges produced larger side forces and rolling moments, with leading edge blowing, than did the model with sharp leading edges.

The research also studied simultaneous blowing from the forebody and wing. The results created forces and moments larger than either forebody or wing blowing alone. The dual blowing achieved the increased forces and increased moments with a $C_{\mu\ wing}$ of 0.02 and $C_{\mu\ body}$ of 0.015.

C. WING/STRAKE BLOWING

1. Miller and Gile

Miller and Gile [Ref. 5] conducted a water-tunnel flow-visualization study of pneumatic blowing on a delta wing undergoing dynamic pitching. As part of the study, data were obtained with blowing off, blowing on, and blowing on while pitching. The delta wings used had leading-edge sweep angles of 60 and 76 degrees and sharp, symmetrically-beveled edges. The blowing jets were introduced to the flow at the 10 percent chord position on centerline or in the vortex core (Figure. 5 [Ref.5]). The 76-degree wing showed the largest improvement in vortex burst delay with blowing (C_{μ} of 0.06) on centerline. At 40 degrees AOA the non-blowing burst location was at the 40

percent chord point; with blowing on, the burst location moved aft to the 100 percent chord location.

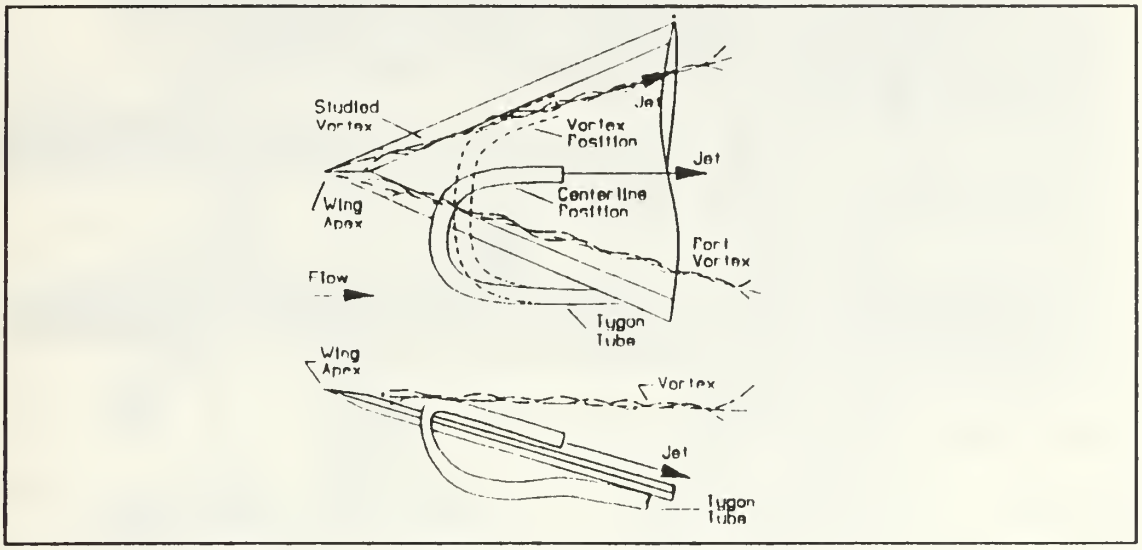

Figure 5. Blowing Jet Positions [Ref. 5]

2. Lemay and Rogers

Lemay and Rogers [Ref. 6] conducted a water-tunnel study to examine the effects of pneumatic blowing on chine/wing vortex coupling (intertwining). Unlike previous research which used rounded forebodies, Lemay and Rogers used a chine forebody. The model was a 4/100-scale generic fighter with a flat-plate, untwisted, uncambered 55-degree cropped delta wing, with sharp leading edges beveled at 45 degrees from the bottom (Figure 6 [Ref.6]). The strake was of gothic planform and beveled in the same manner as the wing. The model also had removable twin vertical tails for examination of their effect on vortex breakdown. Blowing coefficients used were 0.01 to 0.03.

Baseline information for the tailless model showed that the strake vortex initially did not couple with the wing

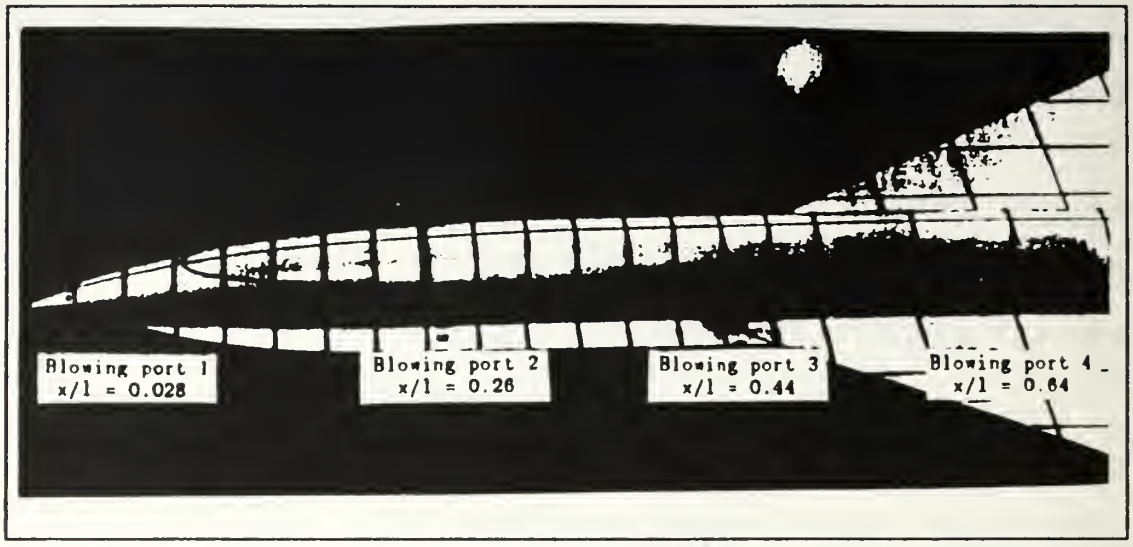

Figure 6. Blowing Port Locations [Ref. 6]

vortex. As the AOA was increased the strake vortex was pulled down under the wing vortex and broke up as it entered the separated flow region and adverse pressure gradient on the wing. With blowing applied the strake vortex was lifted further away from the separated flow region and adverse pressure gradient of the wing. This movement delayed vortex coupling above 24 degrees AOA. The research showed that a blowing coefficient of 0.03 from blowing port 2 (Figure. 7 [Ref. 6]) was sufficient to delay breakdown up to an AOA of 36 degrees. The blowing was also effective in preventing coupling of the vortices up to 33 degrees AOA while the model was in a 5 degree sideslip. Optimal blowing occurred using blowing port 2, a jet sweep angle of 35 degrees, and a jet inclination of 20 degrees.

Not all blowing produced desirable results. Some blowing configurations promoted vortex breakdown. This

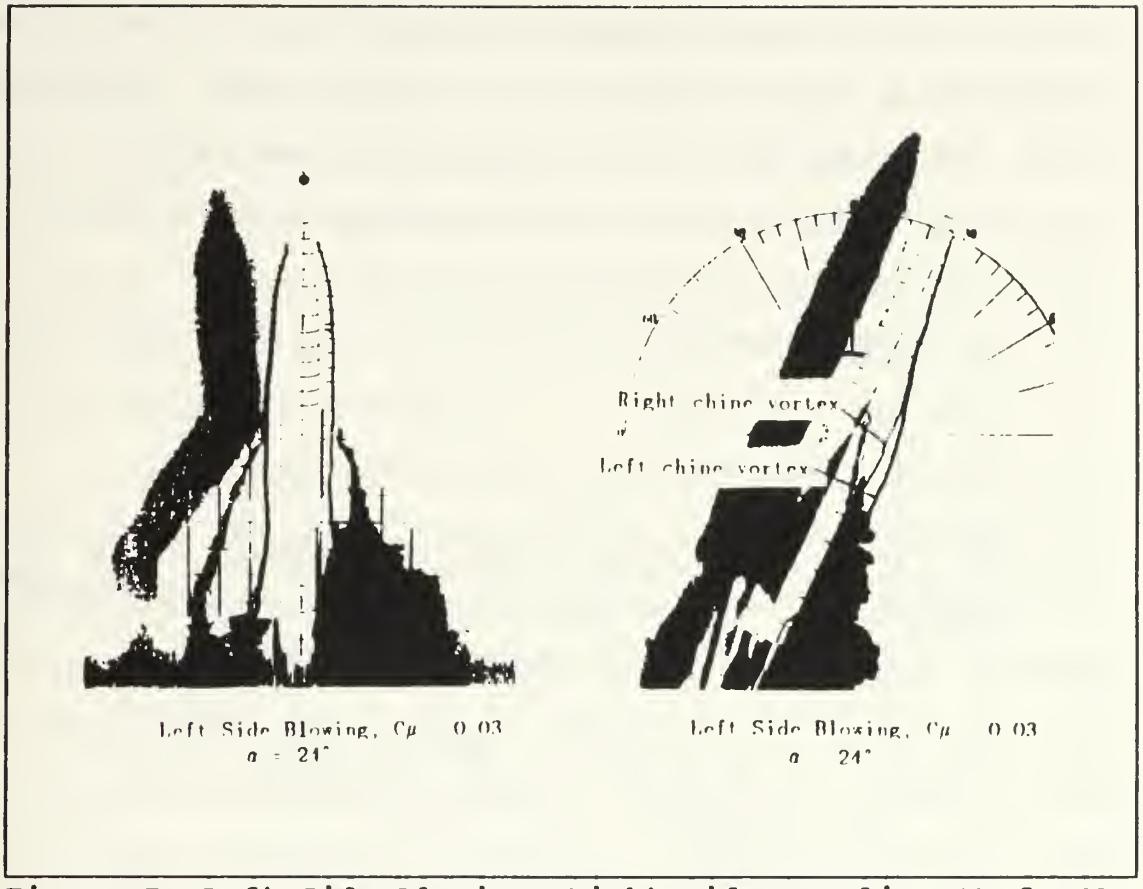

Figure 7. Left Side Blowing, Right Side Coupling [Ref. 6] Blowing Side Vortex Being Lifted Away From Wing

situation typically occurred when blowing from ports behind the strake-wing junction.

3. Roach and Kuhlman

Roach and Kuhlman [Ref. 7, 8] used a laser light sheet and Laser Doppler Anemometry to map the flowfield of LEX vortices and to measure the effects of blowing on the breakdown and coupling locations. The study used an ogive generic-fighter wing-body model consisting of interchangeable strakes and blowing ports (Figure 8 [Ref. 7]). The wing and strake were flat plates with leading edges beveled at 45 degrees. The model provided blowing at four locations on each

side of the fuselage through two different brass blowing tubes with an outer diameter of 0.16 cm (≈ 1/16 inch). Tube 1 was a long tube oriented to blow tangential to the leading edge of the strake, parallel to fuselage, and tube 2 was a short tube angled 35 degrees (sweep angle).

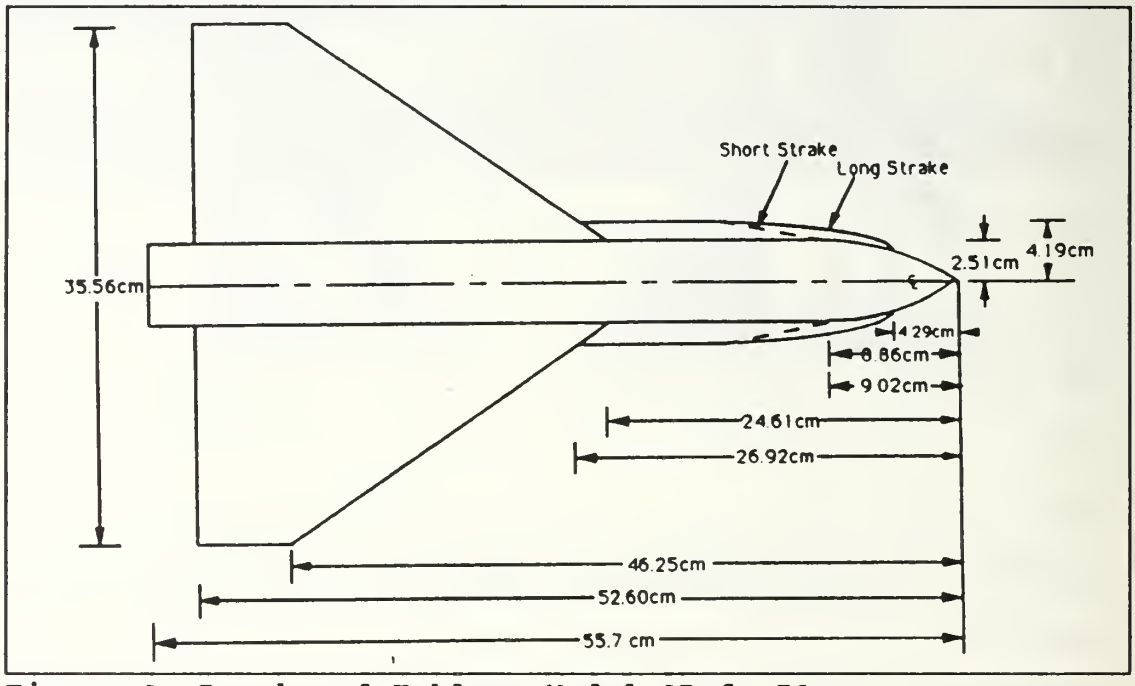

Figure 8. Roach and Kuhlman Model [Ref. 7]

Roach and Kuhlman based their chosen blowing coefficient of C_μ of 0.016 on results obtained by LeMay and Rogers [Ref. 6]. The Roach and Kuhlman study found, through laser-light-sheet flow visualization, that the best delay in vortex breakdown occurred using both the long and short strake with blowing from tube 2 at an inclination of -10 degrees (blowing on the strake top). A favorable delay in vortex breakdown was also produced on the long strake using tube 1 at

port 1 with an inclination of 10 degrees, and on the short strake with tube 1 at port 3 and inclination of 10 degrees.

Flow visualization documented significant reductions in vortex coupling with delays in strake-vortex breakdown. The delay in coupling was attributed to the strake vortex moving away from the wing surface toward the fuselage.

4. Willson and Howard

Willson and Howard [Ref. 9] conducted a quantitative study of the effects on lift and drag of pneumatic wing/strake blowing. They used a half-model generic-fighter fuselage with a wing-strake combination based on the shape used in a study by Kern [Ref. 10]. The wing profile was a NACA-64A008 airfoil, and the strake was wedge-shaped with a sharp leading edge. The surfaces were mounted onto a fuselage with an ogive nose (Figure 9 ,[Ref. 9]). Three interchangeable brass blowing tubes of 0.086 inches I.D. were used in three blowing ports: two on the low-pressure wing side and one on the high-pressure side. The tubes were bent at angles of 30 degrees, 45 degrees, and 60 degrees. The tubes were also able to be adjusted to various inclination angles from -10 degrees to 25 degrees.

Willson was able to demonstrate a maximum of 3.75 percent increase in lift using a C_{μ} of 0.0035 at an AOA of 35 degrees and jet sweep angle of 45 degrees. The peak increase in lift occurred approximately 2.5 degrees AOA after peak C_L values were reached. Their results also showed that while

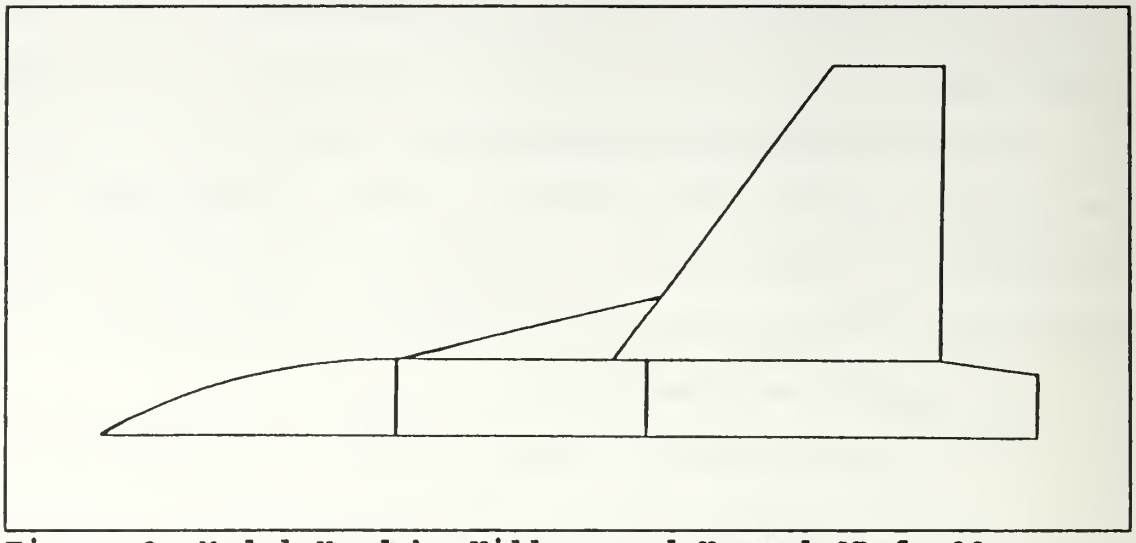

Figure 9. Model Used by Willson and Howard [Ref. 9]

blowing on the high-pressure side increased lift, the largest gains were generated by blowing on the low-pressure side. The study was limited to blowing coefficients below 0.0035, lower than coefficients used by Lemay and Rogers [Ref. 6] and Roach and Kuhlman [Ref. 7,8].

D. KERN'S WING/STRAKE JUNCTION STUDY

Kern, of the Naval Air Warfare Center-Aircraft Division, conducted a numerical investigation on the effects of geometry modifications at the junction of the wing and strake [Ref. 10]. The wing and strake were flat plates with 20-degree beveled edges. The strake had a 76-degree sweep angle and the wing had a 40-degree sweep angle (Figure 10 [Ref. 10]). Three fillets (linear, parabolic, and diamond) were developed to be placed at the wing/strake junction (Figure 11 [Ref. 10]). Kern used two types of computational methods for determining his results. The first method, the Three-dimensional

Euler/Navier-Stokes Aerodynamic Method (TEAM), was used for inviscid flow analysis. The second method, Navier/Stokes Time Dependent (NASTD), developed by McDonnell Aircraft Co., was used for viscous analysis. The Kern study limited its analysis to angles of attack less than 30 degrees.

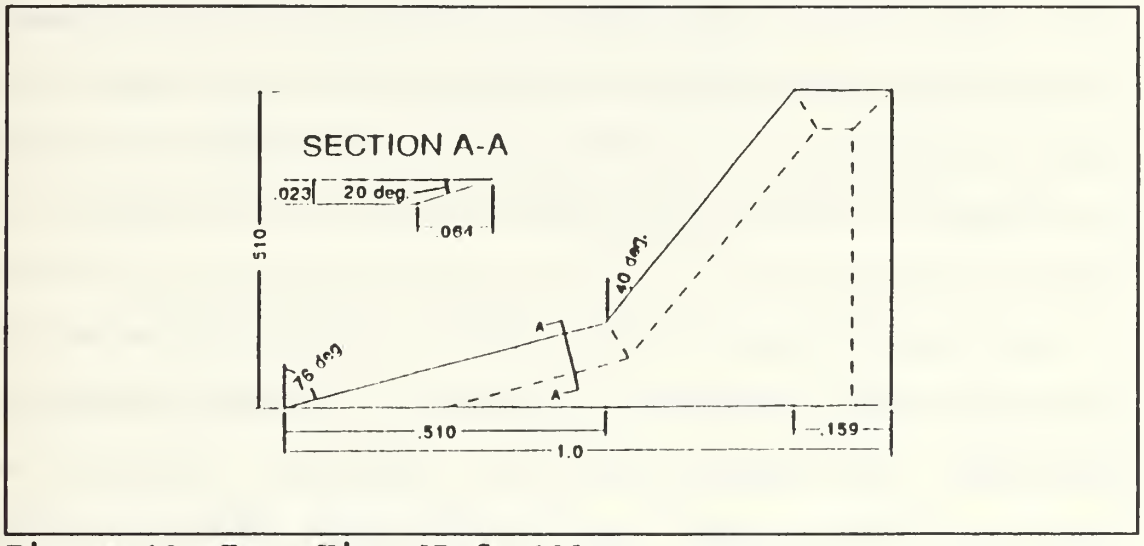

Figure 10. Kern Wing [Ref. 10]

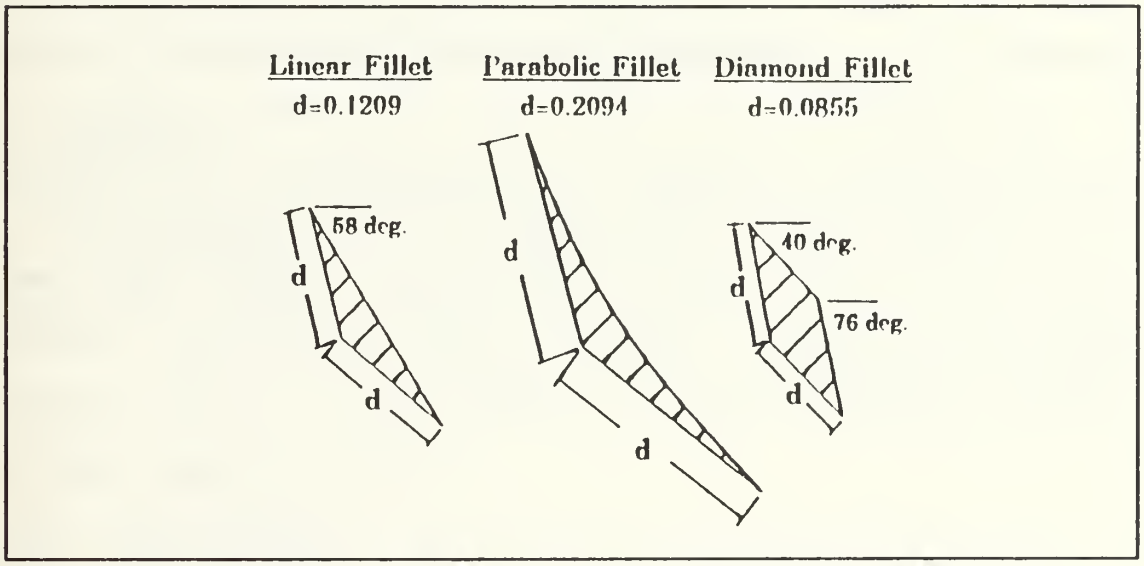

Figure 11. Fillets for Wing/Strake Junction [Ref. 10]

The baseline inviscid analysis at 10 degrees AOA showed two well-defined vortices: one from the leading edge of the strake and the other from the leading edge of the wing. As the AOA was increased the vortices strengthened and the point of coupling of the two vortices moved further upstream. At 22.5 degrees AOA, the predicted cores of the LEX and wing vortices could no longer be distinguished downstream of the intertwining point. The inability to distinguish the cores was caused by a lack of grid resolution in the vicinity of the cores.

The viscous study vortex locations matched those of the inviscous study with one exception. Vortex tearing, a phenomenon not normally seen in numerical studies, was discovered along the wing leading-edge vortex. This phenomenon was caused by the interaction of the wing and strake vortices which created increased coupling.

The diamond-shaped fillet had the greatest effect with angle-of-attack increases. It increased lift by 13.6 percent at 10 degrees AOA and 17.9 percent at 22.5 degrees AOA. The parabolic fillet had the least favorable results, decreasing lift by 4.0 percent at 22.5 degrees AOA.

III. EXPERIMENT AND PROCEDURE

A. OVERVIEW

The research conducted in this experiment is follow-on research to that of Willson and Howard [Ref. 9]. The wing/strake model (to be described shortly) was designed and built at the Naval Postgraduate School (NPS) for use in the NPS low-speed wind tunnel. The half-model was mounted on a reflection plane with normal and axial force measurements made by a wall balance (see Appendix A for calibration procedures). Data were acquired from the signal-conditioning assembly via a multiplexer, amplifier, and analog-to-digital converter. The results were converted to lift and drag forces by the acquisition software, then stored on floppy disks for conversion to lift and drag coefficients.

B. APPARATUS

The equipment used for this research included the NPS low-speed wind tunnel, wing/strake model, mass flow-meter, external strain-gage wall balance, signal-conditioning assembly, balance calibration rig, data acquisition system, and data reduction system.

1. Wind Tunnel

The NPS wind tunnel is a low-speed, closed-circuit, single-return tunnel powered by a 100 hp AC electric motor. The motor is coupled to a three-blade variable-pitch fan

through a four-speed truck transmission (Figure 12). The transmission allows for smooth operation up to 200 mph flow speed. Immediately downstream of the fan is a row of eight stator blades to remove the swirl imparted by the fan. The axial-velocity turbulence level is reduced to 0.2 percent in the test section through a combination of turning vanes in each corner, two fine-wire-mesh screens at the entrance to the settling chamber, and a settling-chamber to test-section contraction ratio of 10:1. [Ref. 11]

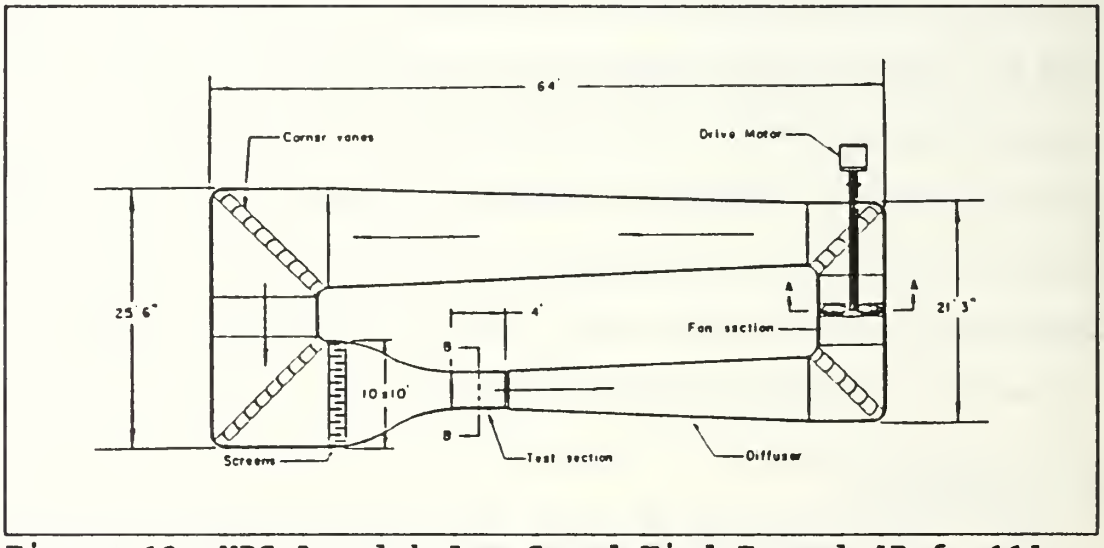

Figure 12. NPS Aerolab Low Speed Wind Tunnel [Ref. 11]

The tunnel static pressure is maintained at approximately atmospheric pressure with breather slots located directly behind the test section. The test section has a cross-sectional area of 8.75 square feet with the reflection plane mounted 4 inches from the bottom. In the center of the reflection plane is a flush-mounted, remotely-controlled turntable capable of varying the AOA in the horizontal plane from -18° to +200°. The turntable is the top of the external

strain-gage balance. Tunnel temperature is obtained by a dial thermometer mounted on the tunnel wall extending into the settling chamber. Corner lighting provided illumination for the test section. [Ref. 11]

The test-section dynamic pressure, q_∞, was determined by measuring the static pressure difference, Δp, between the settling chamber and test section. The pressure differential was measured via a water micromanometer and converted to the test-section dynamic pressure and the test-section velocity using the results of a previous tunnel calibration. Equations 2 and 3 show the conversions [Ref. 12].

$$q_\infty = 2.047(1.1149 \times \Delta p - 0.026749) \qquad (2)$$

$$V_\infty = \sqrt{\frac{2q_\infty}{\rho}} \qquad (3)$$

Where:

ρ	air density (slugs/ft^3)
Δp	micromanometer reading in cm of H_2O
q_∞	test-section dynamic pressure (lbf/ft^2)
V_∞	test-section velocity
2.047	constant converting cm of H_2O to lbf/ft^2
1.1149	tunnel calibration factor
-0.026749	tunnel calibration intercept

The tunnel calibration factor was found by plotting the actual test-section dynamic pressure measured by a pitot-static tube in the test section versus the measured pressure

difference between the settling chamber and the test section [Ref. 12].

2. Wing/Strake Model

The wing and strake were designed for use on a reflection-plane model fuselage previously used in the wind tunnel [Ref 12]. The half-model was fashioned after a generic agile fighter fuselage. The wing/strake used was designed by Willson to match the shape used by Kern [Ref. 10]. Figure 13 shows a sketch of the model. Appendix B contains the geometric parameters for the model.

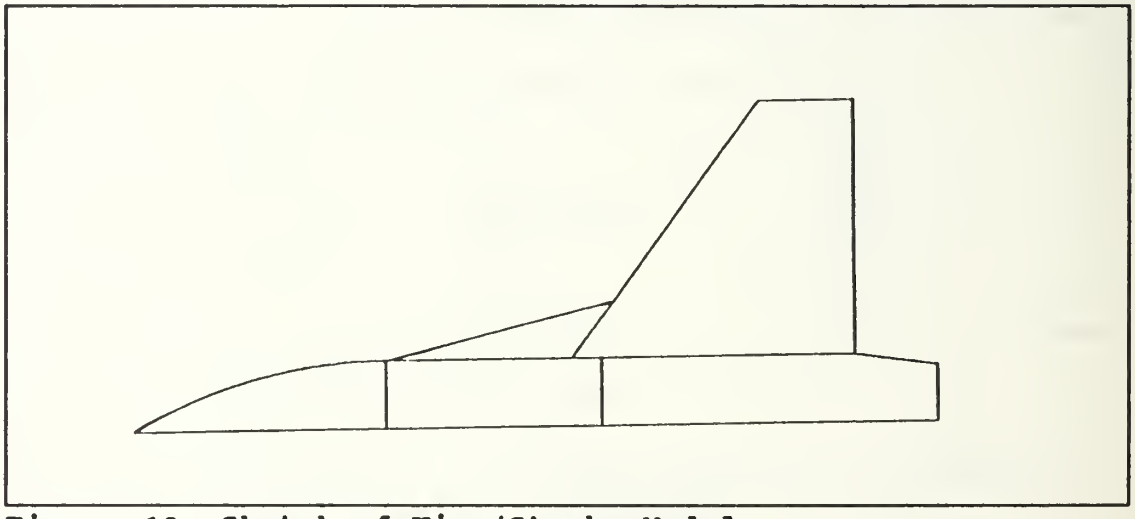

Figure 13. Sketch of Wing/Strake Model

3. Mass Flowmeter and Blowing Apparatus

A Sierra Instruments Model 730 mass flowmeter was used to determine the blowing coefficient, C_{μ}. The system operates on the principle of heat transfer. There are two probes in the flow; one heats the flow while the other measures the temperature increase of the flow. A constant temperature differential is maintained between the probes. The voltage

required to maintain the temperature differential establishes the value for the flow rate. This flow-rate measuring system is independent of input flow temperature or pressure. The flow meter was calibrated to provide a linear readout of 0-5 VDC for mass flows of 0.0 to 0.012486 lbm/s. The accuracy of the flowmeter is ±1 percent of full scale plus 0.5 percent of the reading.

A 125-psi compressor supplied air to three storage tanks. The air was then run from the tanks to the flowmeter through a regulator at a maximum of 65 psi. The air entered the flow meter through a 10-inch-long, 3/4-inch NPT PVC tube. The air exited through a 5-inch-long, 3/4-inch NPT PVC tube (Figure 14). This procedure ensured smooth flow through the flowmeter.

The air then entered a 54-inch-long urethane tube with an inner diameter of 0.125 inches and an outer diameter of 0.375 inches. The tube was attached to a plenum chamber inside the model. The plenum chamber had exit ports for the blowing tubes and for a plenum pressure gage. Fifteen inches of urethane tube ran to the blowing tube at the blowing port.

The blowing tubes were of stainless steel with an outside diameter of 0.125 inches and inner diameter of 0.103 inches. The larger inner diameter, than that used by Willson (0.086 inches), allowed for larger mass-flow rates and higher blowing coefficients. Tube 1 was bent at an angle of 30 degrees, tube 2 at 45 degrees, and tube 3 at 60 degrees

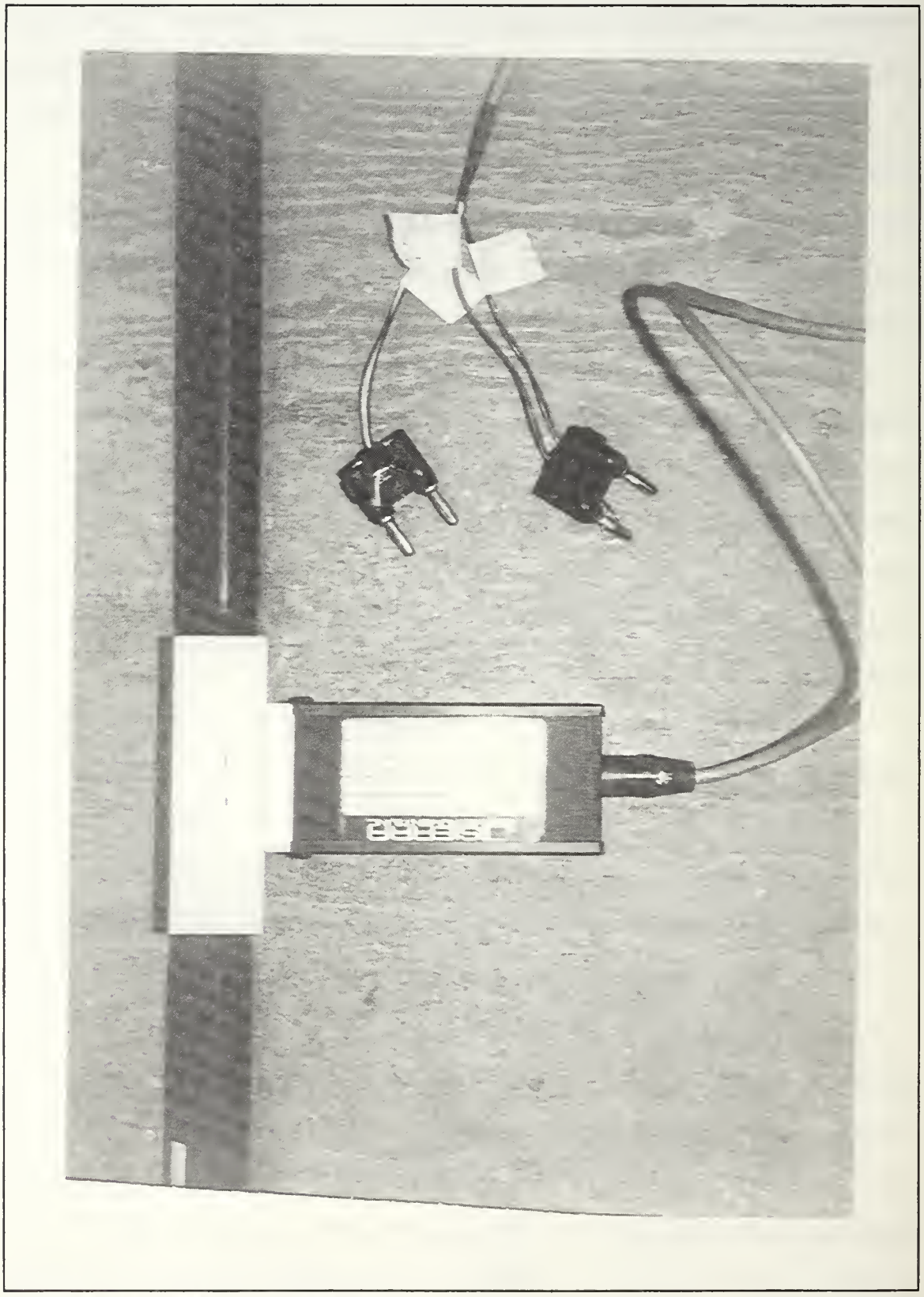

Figure 14. Mass Flowmeter

(Figure 15). The tube angles were based on the results of Roach and Kuhlman, who found optimal blowing with tube angles of 35 degrees and 90 degrees [Ref. 7]. The tube angles in this study provided incremental steps to test for blowing with an angled strake.

Appendix B describes the model and its construction. Blowing tube holes were measured and placed according to the specifications of Willson. Blowing port 1 is the forward-most port on the suction side of the strake. Port 2 is one inch behind port 1. Port 3, on the pressure side, was not used in this experiment and was taped over for all experiments.

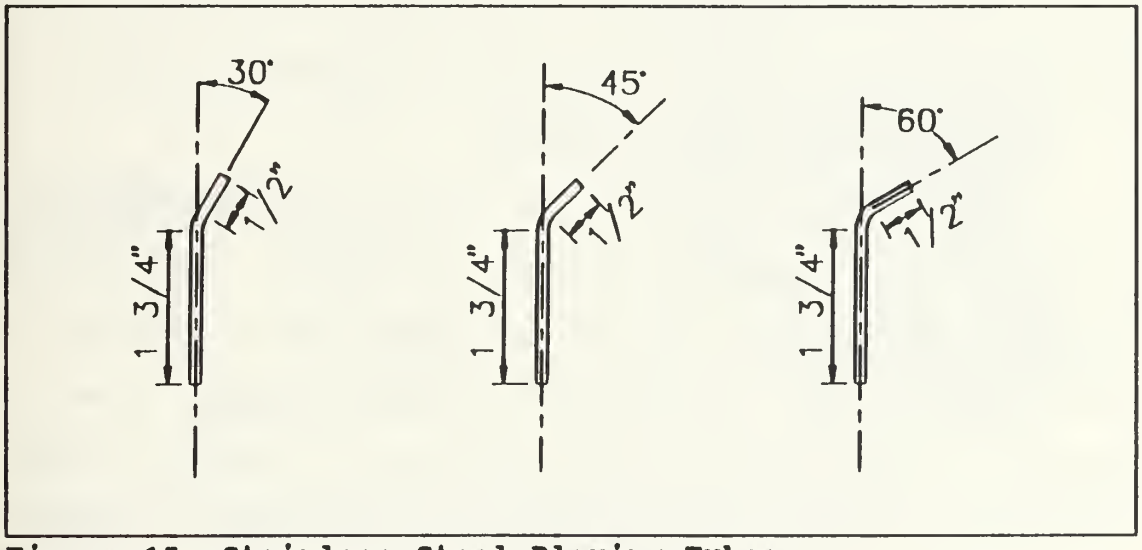

Figure 15. Stainless Steel Blowing Tubes

Blowing coefficients were determined by using equation (1). The voltage readout from the flowmeter was converted to mass flow per second, lbm/s. Jet velocity was verified by calculation to be sonic. The tunnel dynamic pressure was calculated from the water-micromanometer reading.

4. Balance and Turntable

The external strain-gage balance and turntable used in the NPS low-speed wind tunnel was designed and built in 1974 by NPS personnel. It is used for the measurement of normal and axial forces and pitching moments on reflection-plane models. Each strain gage has four active legs for sensitivity and automatic temperature compensation. The normal and axial moments were measured by four orthogonal strain-gage bridges mounted as an integral part of the balance column. Each pair of strain gages are separated by a vertical distance of 26.5 inches. The balance calibration procedures developed by Schmidt [Ref. 13] and Stuart [Ref. 14], and used for this experiment, are discussed in Appendix A.

5. Data Acquisition Hardware

Each strain-gage bridge had an independent voltage supply for its signal-conditioning assembly. Each bridge's signal-conditioning assembly allowed for zeroing and calibration. The differential bridge voltage from each channel's signal-conditioning assembly was passed through a 1000-gain low-noise amplifier then routed to a National Instruments 12-bit MC-MIO-16-9 analog-to-digital (A/D) conversion board that was installed in an IBM P/S-2 computer. The A/D board was capable of 4.88 mV resolution at a gain of one. Figure 16 shows the data acquisition system. [Ref. 9, 13, 14]

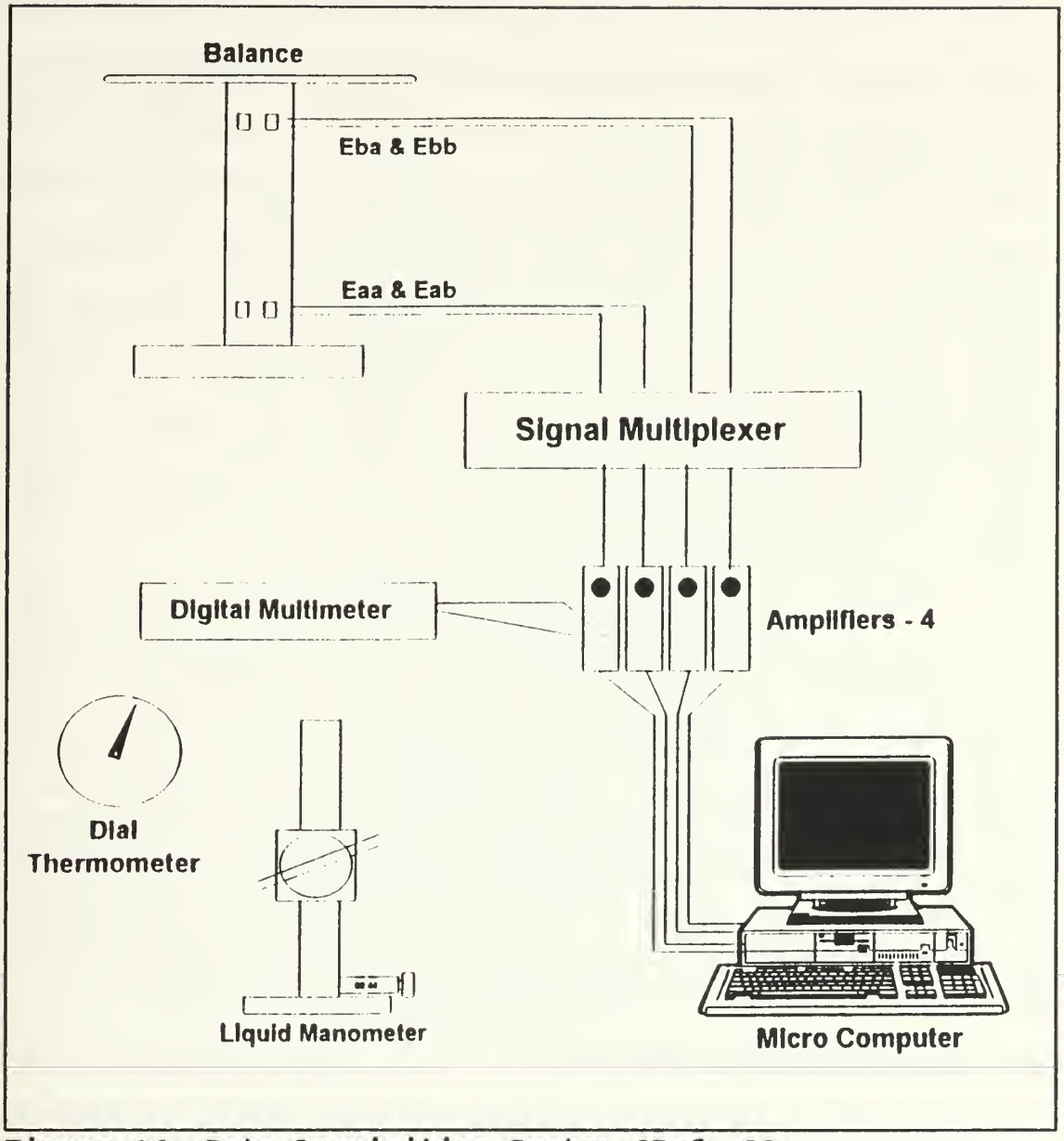

Figure 16. Data Acquisition System [Ref. 9]

6. Data Acquisition Software

The data acquisition software was written in Quick Basic by Willson [Ref. 9]. The program, titled MULTI3.BAS, was a modified version of MULTI2.BAS written by Schmidt [Ref. 13] for a previous study. The program controlled the 12-bit A/D conversion card and the acquisition flow structure. The

software sampled the four channels 1000 times per sample group. Each sample was spaced at 2.25 millisecond intervals, requiring a total sampling time of 2.25 seconds for 1000 samples. The 1000 samples were then averaged to filter high-frequency noise. Noise and internal error were reduced to less than one percent. The averaged channel readings were then used to calculate normal and axial forces using the acquisition software. The software then calculated the lift and drag forces using the data and manually-entered information such as AOA. [Ref. 9]

The files generated by MULTI3.BAS were stored on floppy disk and later manipulated, via spreadsheet, to convert lift and drag forces to coefficient of lift, C_L, and coefficient of drag, C_D, after accounting for corrections due to tunnel blockage, described in Section E. The data acquisition program is listed in Appendix D. Graphs were produced by MATLAB™ after entering the data. [Ref. 9]

C. EXPERIMENTAL CONDITIONS

There were numerous variables that could affect flow separation and vortex formation at high angles of attack. Table 1 lists the parameters, high and low values, for the wind-tunnel runs which were used for data collection.

Wind-tunnel low-frequency fluctuations in velocity were found to occur. The fluctuations grew in intensity as the tunnel temperature rose. Temperatures above 70 degrees led to unacceptable fluctuations. Also noted was that the frequency

TABLE 1.

VELOCITY ft/s	PRESSURE cm H_2O	REYNOLDS NUMBER	MACH NUMBER
135	9.52 9.55	7.599×10^5 8.177×10^5	0.121
125	8.10 8.24	6.990×10^5 7.576×10^5	0.111
112.5	6.59 6.65	6.354×10^5 6.814×10^5	0.101
110	6.25 6.33	6.121×10^5 6.645×10^5	0.098
100	5.20 5.26	5.600×10^5 6.041×10^5	0.089
90	4.21 4.23	5.038×10^5 5.416×10^5	0.080

of the velocity fluctuations increased as the tunnel dynamic pressure was increased.

A 1/5-inch gap was created between the model and the base plate to prevent the two from coming into contact and transferring loads to the reflection plane. Due to the comparative nature of the experiment, there was no correction factor applied to the results for the gap.

Tunnel vibration produced both high and low-frequency noise in the tunnel results. Time-averaging the 1000 readings from the strain-gage bridges recorded in 2.25 seconds effectively filtered out high-frequency random noise. Time-

averaging of 10 or 15 groups of 1000 readings over 25 seconds effectively filtered out low-frequency random noise.

D. EXPERIMENTAL PROCEDURE

1. Pre-run Calibration and Test

Appendix A illustrates the procedure that was used to find the coefficients for the calibration matrices. The procedures are the same as used by Schmidt and Stuart [Ref. 13, 14].

The calibration procedure consisted of hanging weights at two different heights on a rig attached to the rotating plate. Voltage readings were taken at the different weights and heights, then plotted to determine a calibration matrix for use in calculating forces and moments. A pulley apparatus translated the vertical force to a horizontal force on the rig. Figure 17 is a photo of the calibration rig in the tunnel. Prior to loading the rig the IBM-P/S-2 computer was booted and MULTI2.BAS loaded. With the inputs shorted, the Pacific amplifier gain switch was turned to one and the output was adjusted to ± 50 μvolts. The gain was then increased to 1000 and the input adjusted to ± 500 μvolts. The gain on the A/D board was set to one. Channels (2), (4), (6), (8) were read and recorded. The channels were chosen for ease of access to the board. [Ref. 9, 13, 14]

Initially no weight was attached to the calibration rig. MULTI2.BAS prompted the user for the AOA of the model. The displayed axial and normal forces found should have been

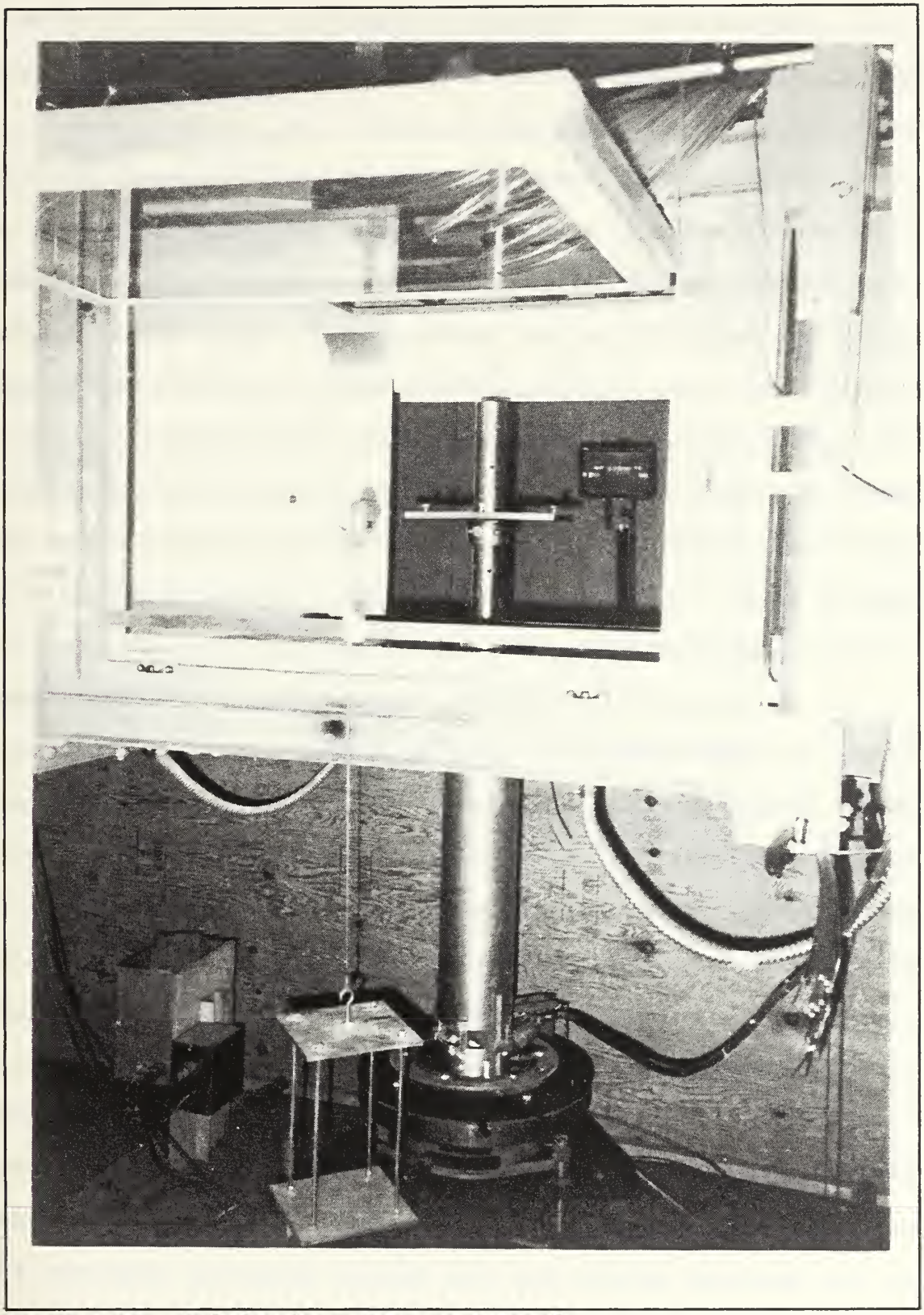

Figure 17. Calibration Rig in Tunnel

less than 0.01 lbf. If the readings were greater, then the offset voltages from channels (2) through (8) were checked and reentered. [Ref. 9, 13, 14]

Once the balance was zeroed, the turntable was rotated to 0 and 90 degrees. The 0-degree position allowed for a pure normal force to be imparted to the balance, while the 90-degree position gave a pure axial force. Successively larger weights were then hung from the balance calibration rig and the normal and axial forces recorded by MULTI2.BAS. A zero-pound tare reading was performed prior to each successive weight application. This procedure eliminated drift from the system. [Ref. 9, 13, 14]

2. Testing Procedures

To ensure a successful experiment, the standardized checklist developed by Willson, with minor modifications, was used. A separate checklist was used for each tunnel run. Any deviations from the checklist, misentered parameters into MULTI3.BAS, or observations critical to the data, were annotated on the back of the checklist. This approach ensured that the data from the files were properly reduced and analyzed. [Ref. 9]

The first step for each tunnel run was to zero the ambient pressure on the water and digital manometers. When this was completed the water micromanometer level was then set to the desired height for the tunnel velocity required for that particular run.

The model was then configured for the test. The blowing tube for the test was installed in the proper port and secured via set screw. Vacant blowing holes were taped over. The air hose was then connected to the flowmeter. Air was turned on and the regulator adjusted to the proper mass-flow rate. The flow was then shut off at the flowmeter with a T-valve. A FOD sweep of the tunnel was performed every day to ensure there were no debris in the tunnel.

The next step was to zero out the amplifiers. The procedures for this step are the same as those in Section D.1, pre-calibration. When this step was completed, the signal from the multiplexer was verified and adjusted as necessary. The zero was set as close to 0.0 μvolts as possible and the span set to 10.0 volts. [Ref. 9]

The final step was to run MULTI3.BAS to test parameters. The program was designed to operate with parallel data files; a different color screen was presented depending on the section of the program being executed. The program first recorded tare values and automatically applied tare corrections to the data. These values were confirmed by taking zero-force readings and verifying the normal and axial force readouts to be less than 0.01 lbf. If the forces were greater than 0.01 lbf, the program was restarted and new tare values recorded. [Ref. 9]

3. Tests Holding C_μ Constant, Varying AOA

The first sets of data collected were for constant C_μ. This was accomplished by setting the output of the flowmeter and tunnel velocity at a constant, and varying the angle of attack of the model. The AOA was varied from 0 degrees to 45 degrees. Non-blowing and blowing data were taken sequentially at each AOA. There were three reasons for choosing this manner of data collection. First, because the tests were of a comparison nature of blowing versus non-blowing, the effect of amplifier drift was extremely minimal over the two and one-half minute total data-collection time, being less than 0.01 lbf/min. Second, due to the ambient temperature being less than 65°F, the tunnel never reached 70°F during one run. Third, Willson had used multiple runs to allow for blowing tares to be taken. It was found that the tares were not required because the blowing jet imparted minimal (< 0.05 lbf) forces on the model. [Ref. 9]

After tares were taken the tunnel was started and the pressure difference was set to the predetermined value in the water micromanometer. Due to the severe weather on the Monterey Peninsula during the winter, the barometric pressure fluctuated from day to day. This caused the water-micromanometer level to have a wide variance to achieve a given tunnel speed; at 125 ft/s the readings ranged from 8.10 to 8.24 cm H_2O. Ten sample groups, of 1000 readings, were taken in 25 seconds for each of the non-blowing and blowing

cases, with the non-blowing data taken before the blowing. The model's AOA was then increased five degrees to the next position. The angle-of-attack sweeps conducted are shown in Table 2. A tunnel velocity of 135 ft/s gave a C_μ of 0.0094, 125 ft/s gave a C_μ of 0.011, 112.5 ft/s gave a C_μ of 0.0136, and 100 ft/s gave a C_μ of 0.0171. A tube inclination angle of 0 degrees was chosen with no previous information for wings with round leading edges.

TABLE 2.

	TUBE 1,30°	TUBE 2,45°	TUBE 3,60°
PORT 1, FWD	135 FT/S 125 FT/S 112.5 FT/S 100 FT/S	135 FT/S 125 FT/S 112.5 FT/S 100 FT/S	135 FT/S 125 ft/s 112.5 ft/s 100 ft/s
PORT 2, AFT	125 ft/s 100 ft/s	125 ft/s 100 ft/s	135 ft/s 125 ft/s 112.5 ft/s 100 ft/s

After each test run was completed the wind tunnel was shut down. When the airflow came to rest, which was confirmed by a zero reading on the digital manometer and stoppage of the fan, three final readings were taken to measure and verify minimal drift. Drift was found never to exceed 0.01 lb/min. The data output files were copied onto a disk and later processed on spreadsheets applying all error corrections.

Once the initial test runs were completed the data were processed. The runs which showed the greatest increase in lift were repeated with a 2.5 degree angle-of-attack increment. The runs were performed for ports 1 and 2 using the 60 degree tube, tube 3. The tunnel velocity was set to 100 ft/s and 125 ft/s. Fifteen sample groups of 1000 readings were used for the repeat tests, with the blowing data being taken before the non-blowing. Taking the blowing data first decreased the time required to obtain all data to a maximum of two minutes.

4. Tests Holding AOA Constant, Varying C_μ

The second test conducted varied C_μ while holding the angle of attack constant. The angle of attack chosen was the one for which the maximum effect of blowing was found: for port 1, 20 degrees; and for port 2, 32.5 degrees. To maximize the C_μ range, for which the upper limit was set by available air pressure and the lower limit by the maintenance of sonic jet velocity, 90 ft/s was chosen. This velocity allowed C_μ's of 0.012 to 0.022 to be tested in 0.001 increments.

After initializing all the equipment and recording the tare values, blowing was turned on and the wind tunnel was started and set to achieve a test-section velocity of 90 ft/s. Fifteen sample groups of 1000 readings were taken, with the blowing data taken before the non-blowing. After each data set the blowing coefficient was adjusted to the new desired value. To secure blowing a T-valve ahead of the flowmeter was

simply closed, saving time between the blowing and non-blowing runs. Total data collection took less than two minutes at each coefficient. Upon completion of the run, the tunnel was shut down and five samples taken to measure and verify minimal drift.

5. Tests Varying Tube Inclination Angle

The final test conducted was one for which the angle of attack and C_μ were held constant, and the tube inclination angle was varied. A tunnel velocity of 110 ft/s was chosen. The angle of attack chosen was again the point of optimal effect of blowing, and C_μ of 0.014 was used. The tube inclination angle was varied from -10 degrees (pointing to the top of the strake) to 40 degrees in 10 degree increments (Figure 18).

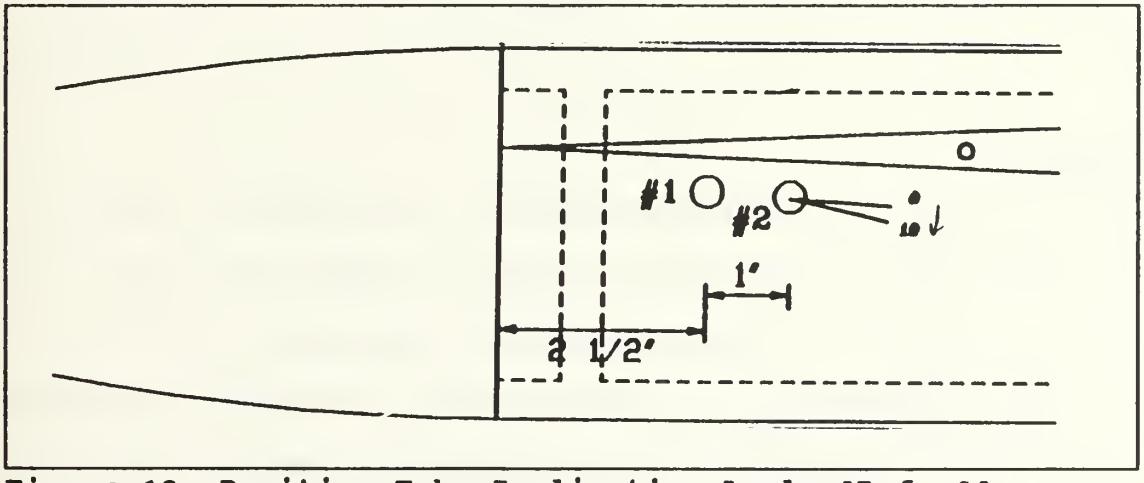

Figure 18. Positive Tube Inclination Angle [Ref. 9]

After initializing all the equipment and recording the tare values, the blowing was turned on and the tunnel started and set for 110 ft/s. Fifteen sample groups of 1000 readings were taken for blowing and non-blowing cases. Again, each

data series required less than two minutes for completion. To adjust the tube angle, the tunnel velocity was brought to zero. The tube angle was adjusted to the new desired value, and the tunnel speed again set. Upon completion the tunnel was secured and five samples taken to measure and verify minimal drift.

E. EXPERIMENTAL CORRECTIONS

Wind tunnel testing requires that certain corrections to the lift and drag measurements be made. The corrections applied were wake blockage and solid blockage. These corrections were made as part of the spreadsheet data reduction process. The total solid blockage and wake blockage are represented by: [Ref. 9]

$$\varepsilon_t = \varepsilon_{sb} + \varepsilon_{wb} \qquad (4)$$

Where:

ϵ_t	total blockage correction
ϵ_{sb}	solid blockage correction
ϵ_{wb}	wake blockage correction

For models where corrections can not easily be derived, the total blockage may be estimated by: [Ref. 11]

$$\varepsilon_t = \frac{1}{4} \times \frac{Model\ Frontal\ Area}{Test\ Section\ Area} = 0.04156 \qquad (5)$$

Equation (6) is the equation used for the blockage correction during this study. The blockage factor, ϵ_t,

obtained from equation (5) and (7) was then applied to the lift and drag coefficients by correcting the dynamic pressure (q_∞) using equation (6). [Ref. 12]

$$q_{corr}=q_\infty(1+\varepsilon_t) \qquad (6)$$

Where:

q_{corr}	corrected dynamic pressure
q_∞	determined dynamic pressure

The model frontal area is a function of angle of attack. The axial cross-sectional area is small, 0.110 ft^2 compared to the longitudinal area, thereby only the longitudinal cross-sectional area was used. The model's longitudinal cross sectional area was determined to be 1.4545 ft^2. Using the wind tunnel cross sectional area of 8.75 ft^2, and equation 6, the total blockage correction became: [Ref. 9]

$$\varepsilon_t=0.04156\times SIN(AOA) \qquad (7)$$

As noted in Section C, the tunnel had a periodic rise and drop in velocity. This rise had an amplitude of approximately 0.05 cm of H_2O in the water micromanometer as did the drop. The duration of the velocity rise was 4 to 5 seconds, with 20 to 25 seconds between increases. The velocity drop occurred at the same amplitude and frequency. To offset the velocity oscillations, ten sets of 1000 voltage readings were used for preliminary data collection, increased to 15 for final data collection. [Ref. 9]

IV. DISCUSSION AND RESULTS

A. OVERVIEW

This section discusses the results obtained from this study. The study consisted of three types of tests described in Chapter III, Sections D.3, D.4, and D.5. Data collected was imported into Microsoft Excel 4.0 for Windows™ where the individual samples of each sample group were collected and averaged. Blockage corrections were also applied through Excel™.

B. BASELINE MODEL PERFORMANCE

The model used in this study is patterned after the NAWC-AD study by Kern. Therefore, a comparison of the baseline results is required. Figure 19 is the model's lift-curve. The curve shows the linear lift-curve slope from 0 to 22.5 degrees AOA. Above 22.5 degrees AOA the wing began to stall. The strake vortex extending over the wing began to generate lift, and at 35 degrees was the dominate lift generator. The wing maintains a minimum C_L of 1.4 until 50 degrees. Above 50 degrees AOA the curve drops off due to vortex breakdown [Ref. 9]. A wing reference area of 0.969 ft^2 (projected through the model fuselage) was used for all coefficient calculations.

Figure 20 [Ref. 10] shows the lift-curve for the Kern study. The wind-tunnel model had a higher maximum lift and steeper lift-curve slope, $C_{L\alpha}$, than the Kern computer model.

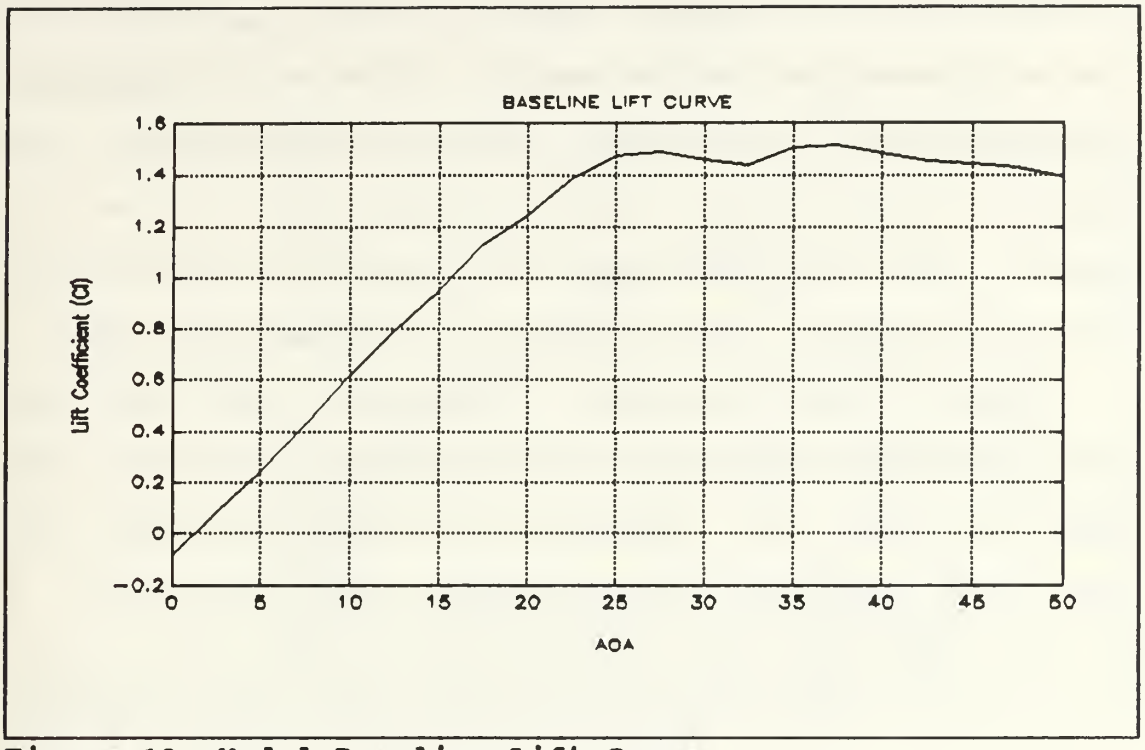

Figure 19. Model Baseline Lift Curve

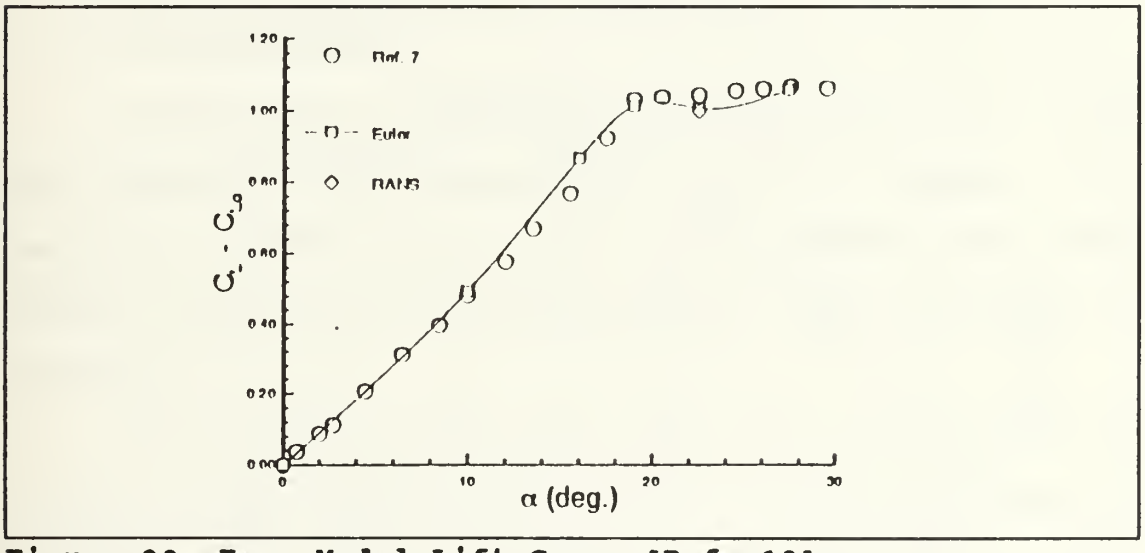

Figure 20. Kern Model Lift Curve [Ref. 10]

This difference can be attributed to the computer model having sharp leading edges and the wind-tunnel model having a round leading edge. The wind-tunnel model also had a fuselage which contributed to the lift. $C_{L\alpha}$ for the wind-tunnel model was

0.0616/deg, while the Kern computer model's $C_{L\alpha}$ was 0.05/deg. Also affecting the results was the lack of wall interference correction tending to make the lift-curve slope steeper. Both Figures 19 and 20 show a relatively flat curve in the stall region. The wind-tunnel model stalled at 22.5 degrees AOA, while the computer model stalled at 19 degrees AOA. [Ref. 10]

Figure 21 shows the model's drag polar. The wind-tunnel model performed comparable to the computer model below stall, Figure 22 [Ref. 10]. However, the wind-tunnel model had a higher lift per drag than the computer model above stall. C_{Do} for the model was 0.055, while the Kern model had a C_{Do} of

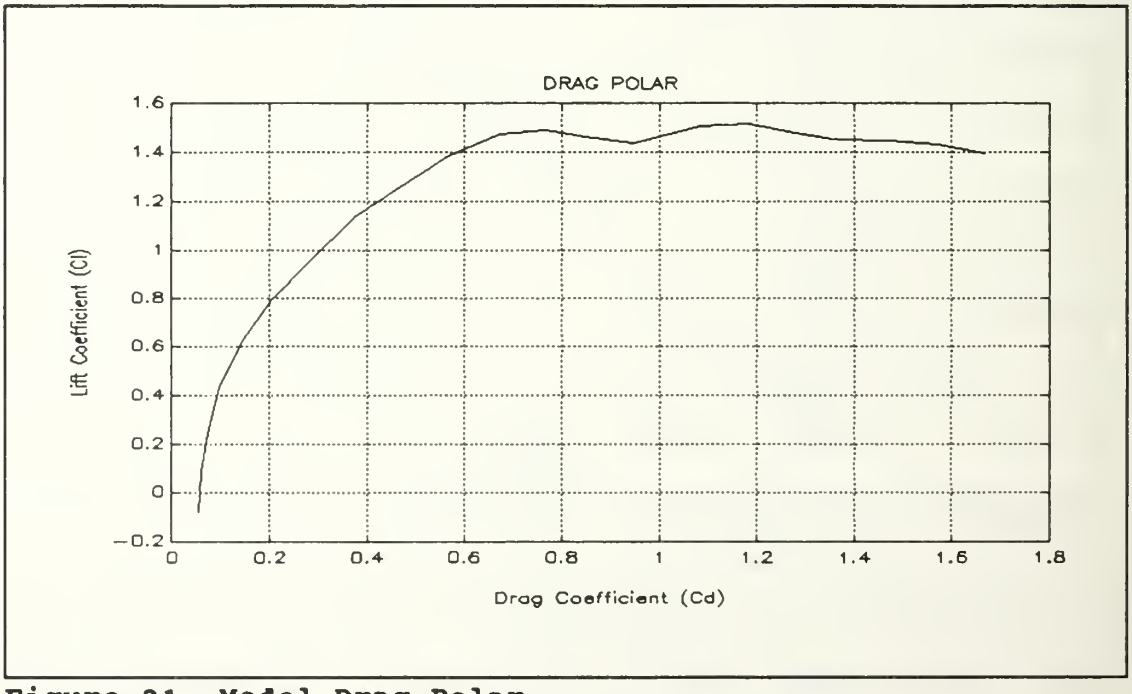

Figure 21. Model Drag Polar

0.02. The wind-tunnel model had a higher C_{D_0} because it had a fuselage and attached urethane air supply tubes.

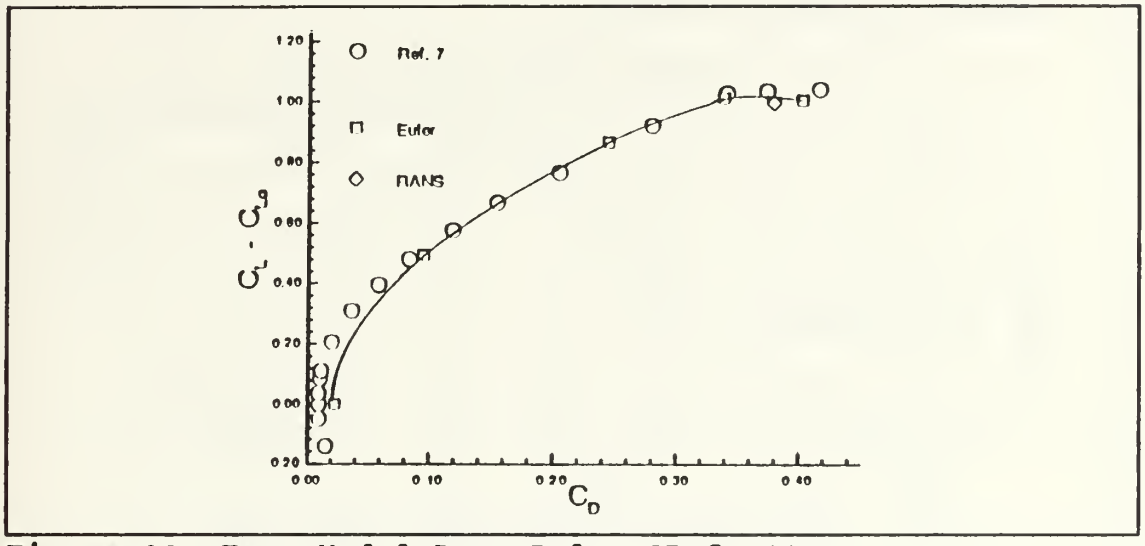

Figure 22. Kern Model Drag Polar [Ref. 10]

C. TESTS HOLDING C_μ CONSTANT VARYING AOA

1. Blowing Port 1

These test were performed at four different C_μ's using each of the three blowing tubes at 0-degrees incidence. Only the most favorable results will be discussed. Additional figures containing data from non-optimal runs are included in Appendix C.

The first step in this study was to determine an optimum C_μ and blowing tube angle. One experiment was performed for each of the points indicated in Table 2, Chapter III, Section D.3. The optimal results for blowing port 1 were using blowing tube 3 and a C_μ of 0.017. Figure 23a and 23b show the lift and the percentage increase in lift gained

through blowing. Figures 24a and 24b show the lift and percentage increase for a C_μ of 0.011.

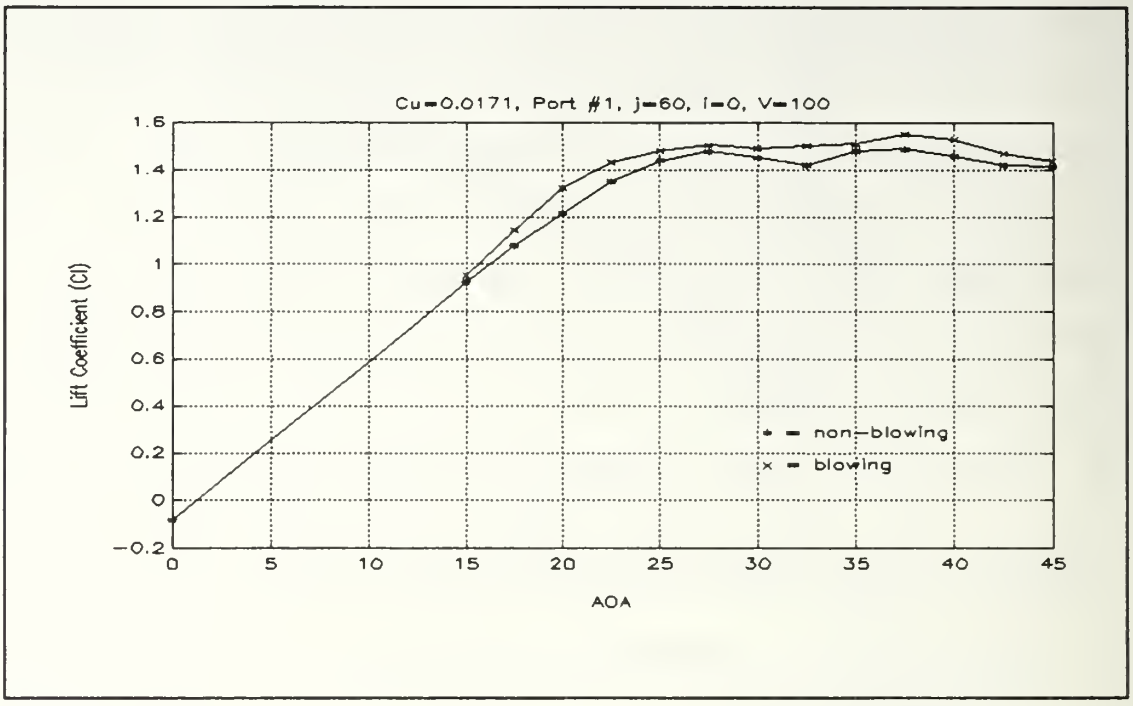

Figure 23a.

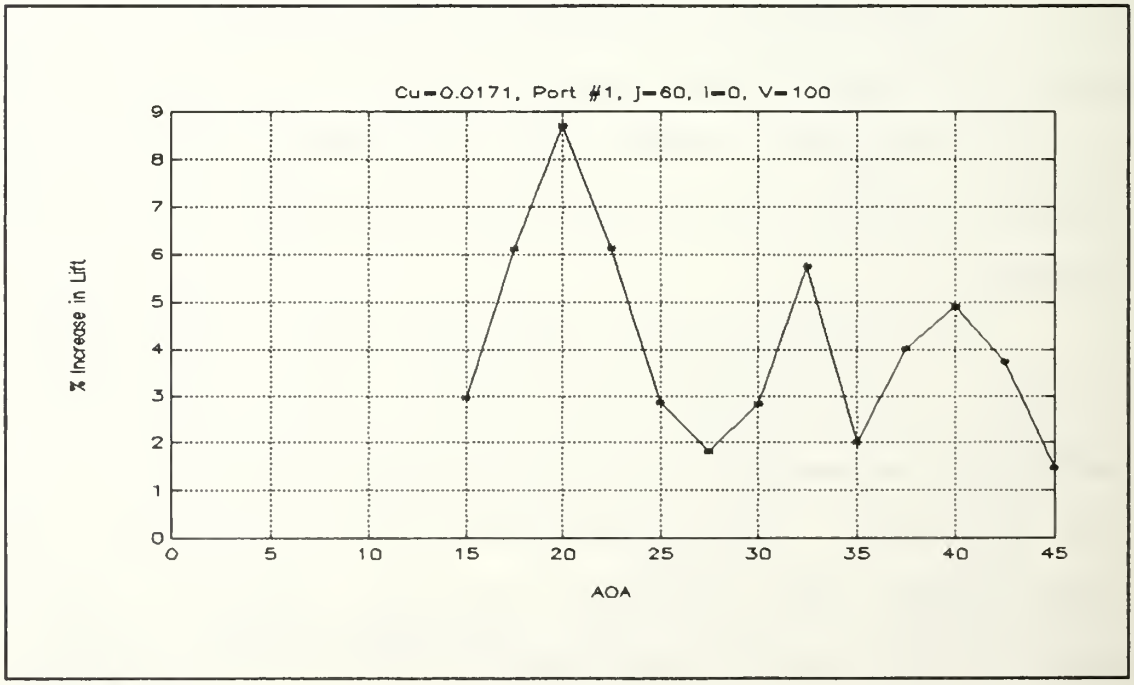

Figure 23b.

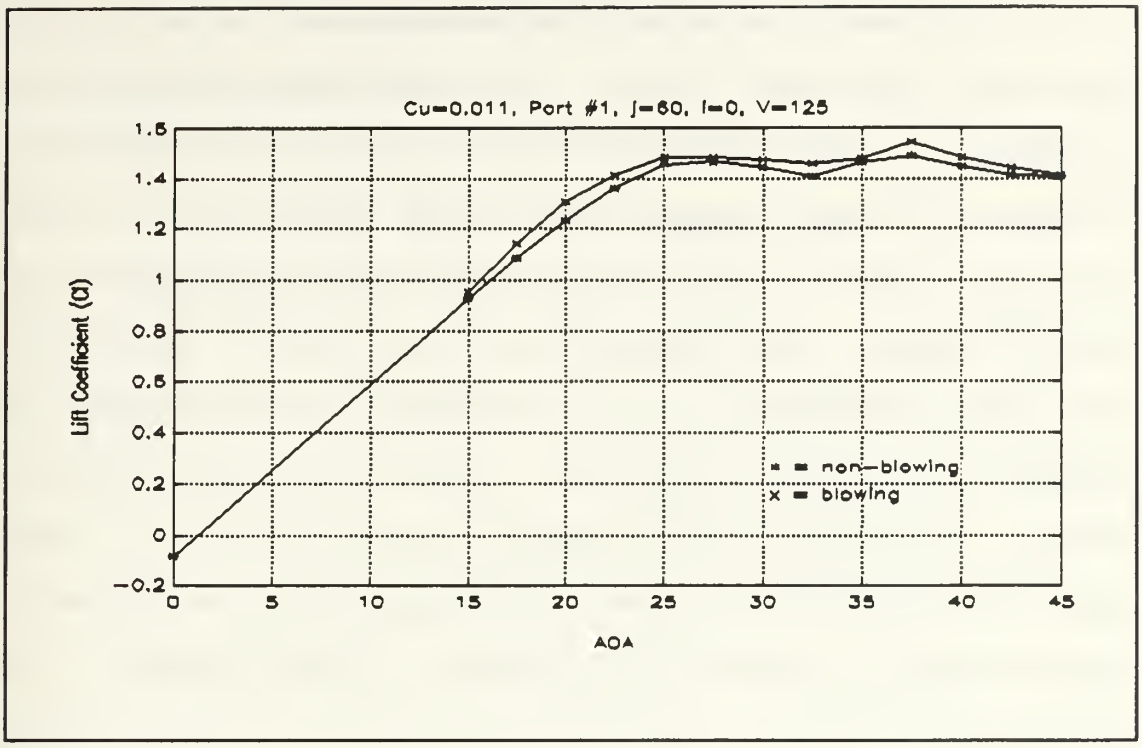

Figure 24a.

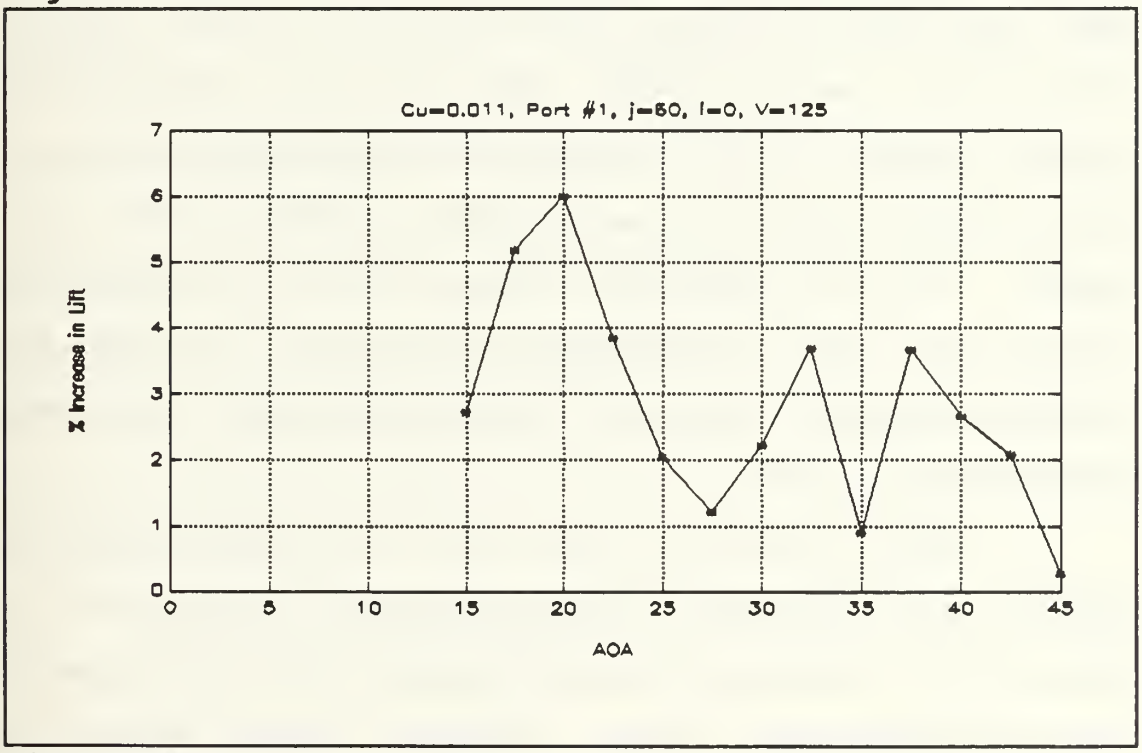

Figure 24b.

Figures 23a and 24a show an increase in lift across the entire AOA range studied, with peaks at 20 degrees and 32.5 degrees. The third peak in the figures are separated by 2.5 degrees. The increase effect at 20 degrees was probably due to the initial weak strake vortex being strengthened by the blowing jet. Flow visualization done by Roach and Kuhlman found that blowing with a C_μ of 0.016 at 20 degrees AOA delayed strake-vortex breakdown location by approximately 50 percent of the non-blowing breakdown location [Ref. 7]. Their study found that blowing moved the strake vortex away from the wing surface and towards the fuselage. This movement of the strake vortex delayed coupling with the wing vortex. As the angle of attack increased the point of vortex coupling (intertwining) moved forward. The oscillatory nature of the percent increase in lift was possibly due to direct effect of strake-vortex movement plus reattaching effect in the stall region. Flow visualization is required to determine the extent of the vortex interaction and coupling. The data also indicate that the larger the blowing coefficient the greater the increase in lift.

Figure 25 shows the drag curve for the conditions in Figure 23a. There was a slight increase in drag above 35 degrees AOA. The largest increase occurs at the third peak of the percent increase curve. However, there was not an increase in drag at the other peaks as might be expected. As

data indicated no appreciable change in drag, it will no longer be discussed.

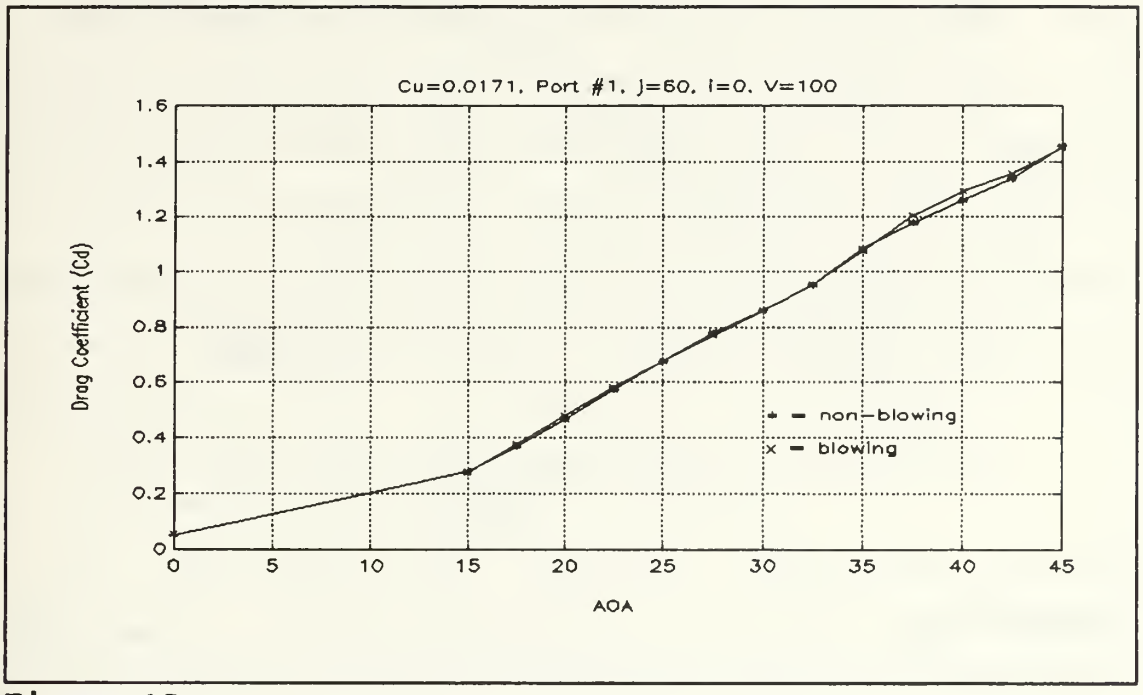

Figure 25.

2. Blowing Port 2

One experiment was performed at each of the points indicated in Table 2, Chapter III, Section D.3. Optimal results for port 2 were obtained using blowing tube 3 with a C_μ of 0.017. Figures 26a and 26b show the lift and percentage increase curves for the wind-tunnel model with and without blowing turned on.

Figures 26a and 26b show a marked increase in lift over the entire AOA range studied, with peaks at 20 degrees, 32.5 degrees, and 40 degrees. These peaks match those in Figures 23a and 23b, though the amplitude of the peaks have different values. Blowing port 2 appeared to increase the

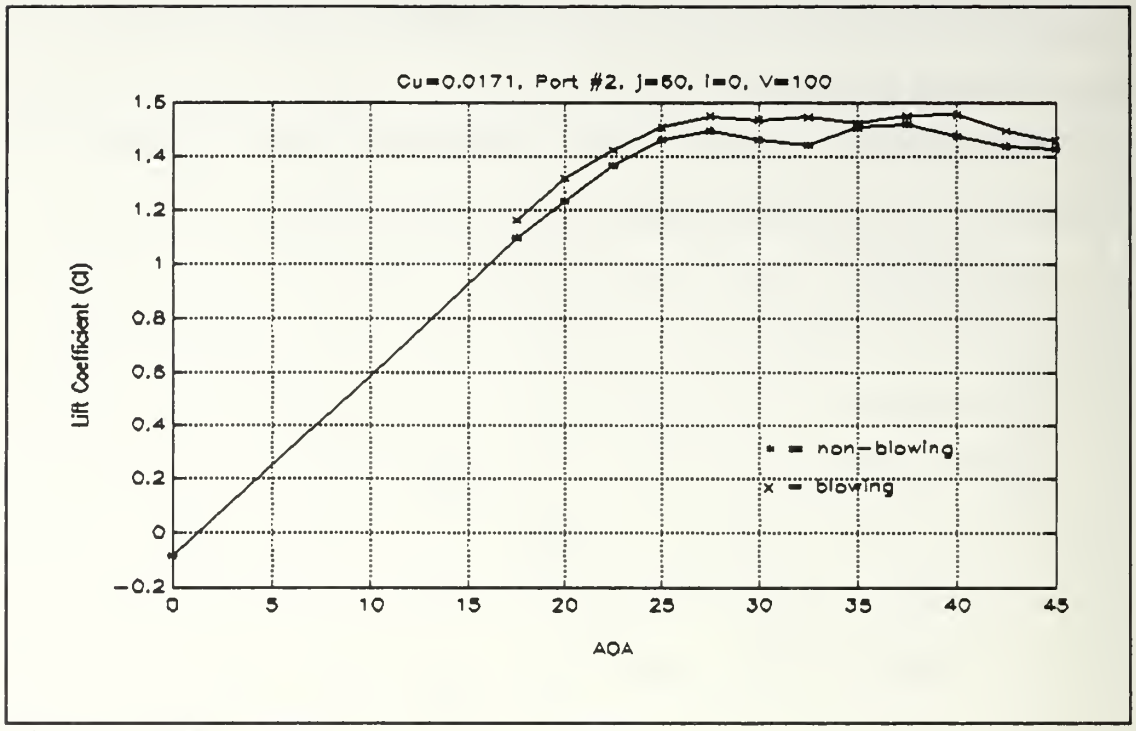

Figure 26a.

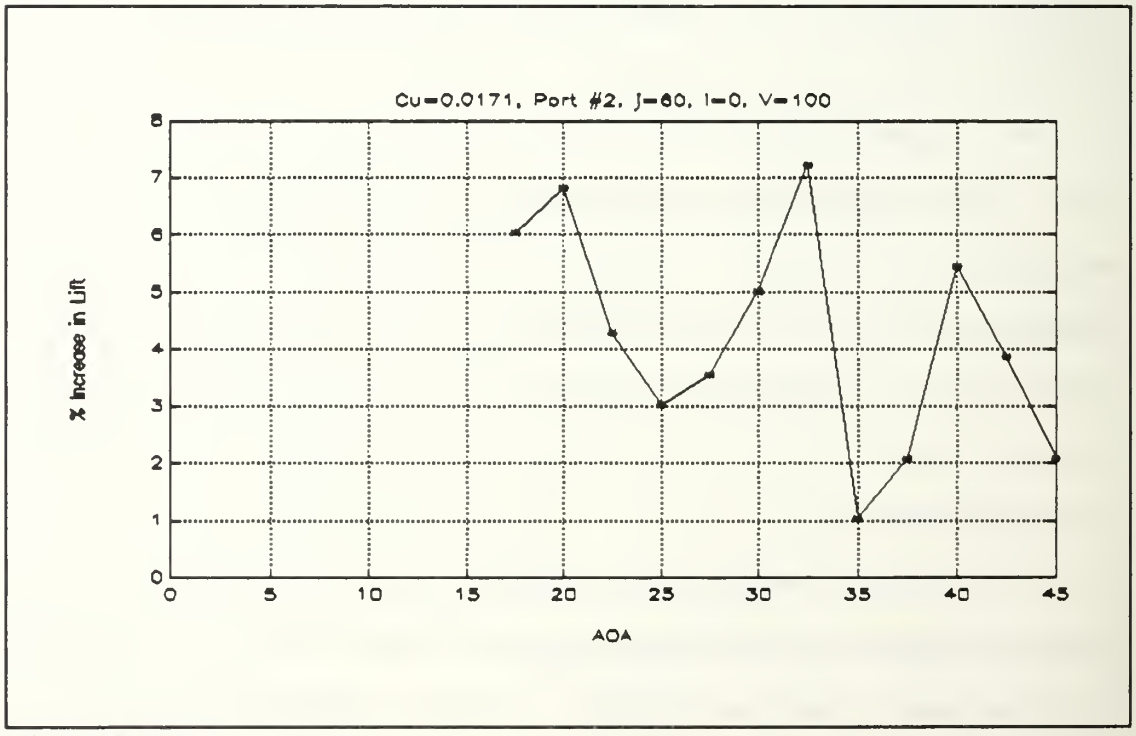

Figure 26b.

peaks at 32.5 degrees and 40 degrees, while decreasing the peak at 20 degrees. The greater increase in lift at the high angles of attack was probably due to the strake vortex being strengthened further back on the strake/wing. The data indicated that moving the blowing port aft may increase the AOA at which the maximum ΔC_l occurs. However, based on data from Lemay and Rogers, an aft limit will be reached for which moving the blowing port back no longer produces desirable results [Ref. 6].

D. TESTS HOLDING AOA CONSTANT, VARYING C_μ

Two experiments were conducted varying the blowing coefficient. One was performed with blowing at port 1, and one with blowing at port 2. Figures 27a and 27b show the lift-curve and percentage increase in lift for port 1, tube 3, and AOA of 20 degrees. Figures 28a and 28b show the same information for port 2, tube 3, AOA of 32.5 degrees. The AOA chosen was the one for which the maximum effect of blowing was found from the previous data.

All the figures confirm the data of Section C. An increase in the blowing coefficient lead to an increase in lift over the range tested. Figures 27b and 28b also indicate that the lift increase was directly proportional to the blowing coefficient increase.

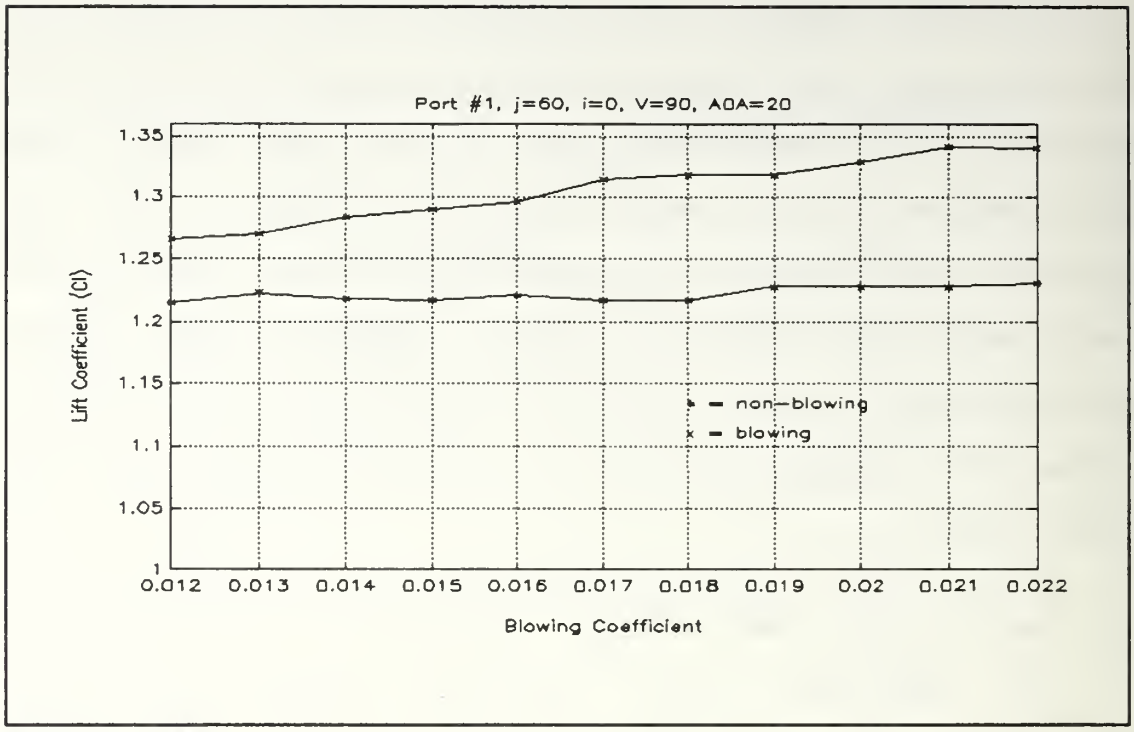

Figure 27a.

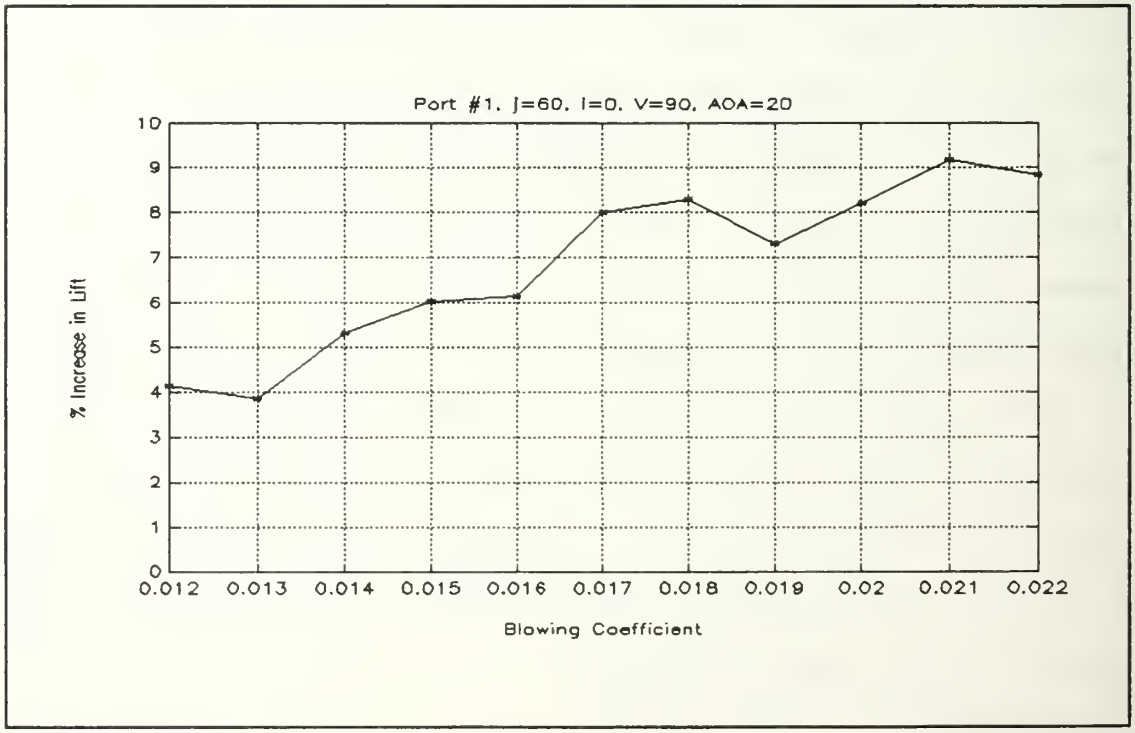

Figure 27b.

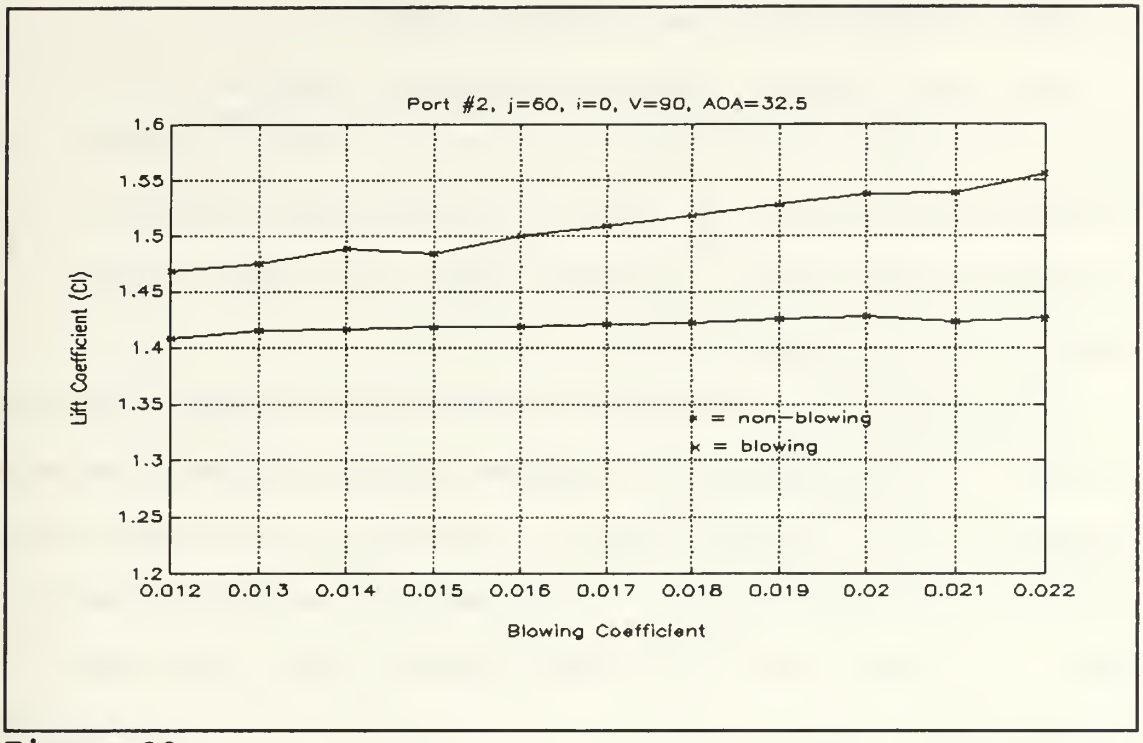

Figure 28a.

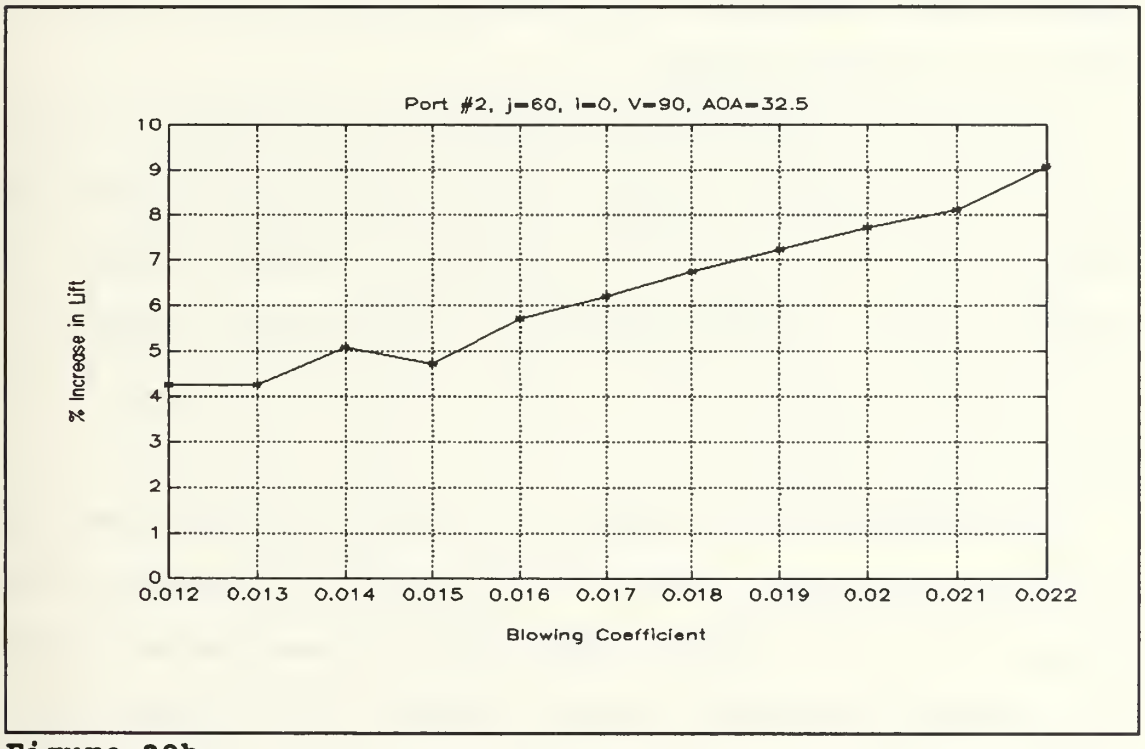

Figure 28b.

E. TESTS VARYING TUBE INCLINATION ANGLE

Two experiments were performed varying the tube inclination angle at each blowing port. The AOA chosen was the same as in Section D, the one for which the maximum effect of blowing was found. Blowing tube 3 was used because it generated the maximum increase in lift.

Figures 29a and 29b show the lift and percentage increase in lift for blowing port 1. Figures 30a and 30b show the same information for blowing port 2. Blowing at an inclination angle of 0 degrees at port 1 produced the greatest increase in lift. As can be seen from Figure 29b, the range of inclination angles between -10 degrees and 20 degrees significantly increased lift while those greater than 20 degrees had minimal effect.

Blowing at an inclination angle of 10 degrees at port 2 produced the largest increase in lift. As can be seen from Figure 30b, the range of inclination angles between -10 degrees and 30 degrees produced a significant increase in lift. Those angles greater than 30 degrees showed a much smaller lift increase.

The reason for the increase in inclination angle required to produce optimum lift as the blowing jet source moves further aft is not known. More locations need to be studied to determine the optimal blowing location for a given AOA.

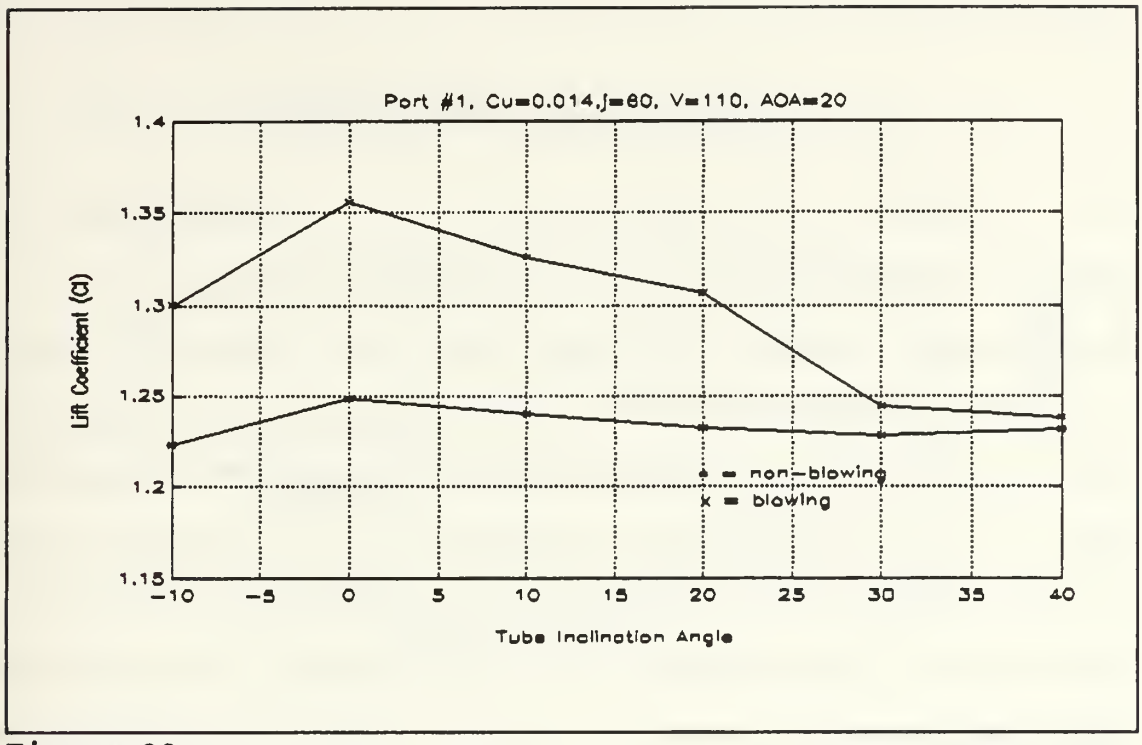

Figure 29a.

Figure 29b.

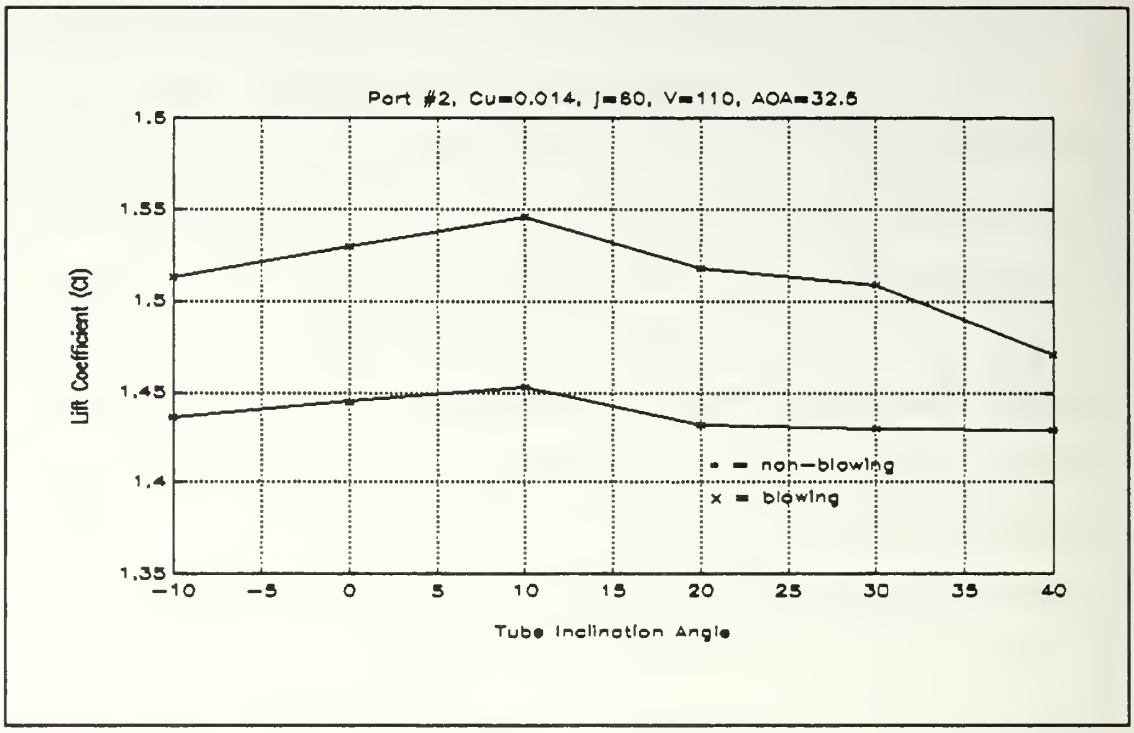

Figure 30a.

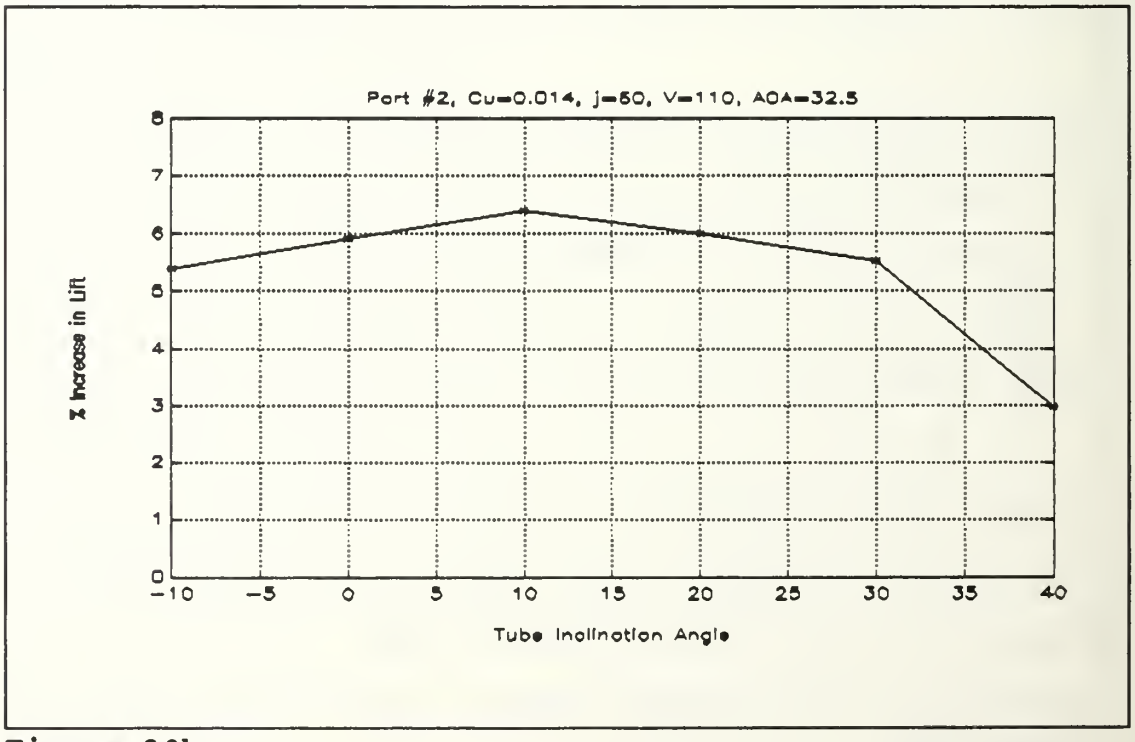

Figure 30b.

V. CONCLUSIONS AND RECOMMENDATIONS

A. CONCLUSIONS

The wing/strake mounted to the generic-fighter half model showed improved lift when pneumatic blowing was applied. Blowing from port 1, at a C_μ of 0.0171, improved lift 8.75 percent at 20 degrees AOA, 5.75 percent at 32.5 degrees AOA, and 4.9 percent at 40 degrees AOA. Blowing from port 2, at a C_μ of 0.0171, improved lift 6.8 percent at 20 degrees AOA, 7.3 percent at 32.5 degrees AOA and 5.4 percent at 40 degrees AOA. The oscillatory nature of the increase was probably due to the local dynamics of vortex formation and flow separation.

The data indicated that the higher the blowing coefficient the greater the lift increase. Over the coefficient span tested, 0.012 to 0.022, the increase in lift was linearly proportional to the increase in blowing. A wider range of blowing coefficients was not pursued.

Blowing at port 1 produced the largest lift increase at 20 degrees AOA, while blowing at port 2 produced the largest lift increase at 32.5 degrees AOA. The data indicated that an increase of AOA for peak lift enhancement with aft movement of blowing location may occur. However, there is probably an aft limit beyond which the results will deteriorate. Lemay and Rogers found that blowing behind the wing/strake junction

produced negative results [Ref. 6]. This research did not investigate blowing ports aft of port 2.

Blowing tubes 1 (30 degrees) and 2 (45 degrees) did not produce the significant increases in lift as did tube 3 (60 degrees). Tube 2 did improve lift more than tube 1. The data indicated the greater the tube angle the greater the lift increase for the values tested.

There was an optimum blowing tube inclination angle for each blowing port. The optimum angle for port 1 was 0 degrees, and for port 2 was 10 degrees. The angles between -10 degrees and 20 degrees for port 1, attained a minimum value of 71 percent of the increase at 0 degrees. The angles between -10 degrees and 30 degrees for port 2, attained a minimum value of 85 percent of the increase at 10 degrees. The data indicated that tube inclination angle was not as important as blowing jet angle, and should be examined last when trying to optimize pneumatic blowing.

B. RECOMMENDATIONS

Two more blowing tubes should be made with angles of 75 degrees and 90 degrees. These tubes would allow further examination of jet-tube angle versus the increase in lift.

An additional port, or ports, should be added to the model aft of port 2. These additional ports would be used to examine the increase in AOA at which maximum lift increase occurs.

A flow visualization study needs to be made of the wing/strake flowfield. This study may indicate the cause for the oscillation in lift increase on the wing. The results can also be compared to the results of Roach and Kuhlman. The comparison may indicate that strake design has an influence on the success of wing/strake pneumatic blowing. A water-tunnel study of a smaller scale model may be compared to the results of Lemay and Rogers. The results could also be used to determine the influence of strake design on pneumatic blowing results.

Fillets should be designed for the model. The fillets would allow for a comparison of lift increase on the model with the results obtained by Kern [Ref. 10]. The fillets would also give a baseline performance so that research into pneumatic blowing with the fillets in place could be conducted.

LIST OF REFERENCES

1. LeMay, S. P., Sewall, W. G., Henderson, J.F., *Forebody Vortex Control on the F-16C using Tangential Slot and Jet Nozzle Blowing*, AIAA Paper 92-0019, January 1992.

2. Guyton, R. W. and Maerki, G., *X-29 Forebody Jet Blowing*, AIAA Paper 92-0017, January 1992.

3. Cornelius, K. C., Pandit, N., Osborn, R. F.,Guyton, R. W., *An Experimental Study of Pneumatic Vortex Flow Control on High Angle of Attack Forebody Model*, AIAA Paper 92-0018, January 1992.

4. Celik, Z. Z. and Roberts, L., *Aircraft Control at High Alpha by Tangential Blowing*, AIAA Paper 92-0021, January 1992.

5. Miller, L. S. and Gile, B. E., *The Effects of Blowing on Delta Wing Vortices During Dynamic Pitching at High Angles of Attack*, AIAA Paper 92-0407, January 1992.

6. LeMay, S. P. and Rogers, L. W., *Pneumatic Vortex Control on a 55 Degree Cropped Delta Wing with Chined Forebody*, AIAA Paper 90-1430, June 1990.

7. Wright Laboratory Final Report WL-TR-91-3065, *Experimental Investigation of the Effects of Blowing on Bursting of Strake Vortices*, by R. A. Roach, and J. M. Kuhlman, July 1991.

8. Roach, R. A. and Kuhlman, J. M., *Strake Vortex Conntrol Using Pneumatic Blowing*, AIAA Paper 91-3274-CP, 1991.

9. Willson, J. G., *Quantitative Force Measurements of Pneumatic Control on a Wing/Strake Model*, Master's Thesis, Naval Postgraduate School, Monterey, Ca., September 1992.

10. Kern, S. B., *Numerical Investigation of Vortex Flow Control Through Small Geometry Modifications at the Strake/Wing Junction of a Cropped Double Delta Wing*, AIAA Paper 92-0411, January 1992.

11. *NPS Laboratory Manual for Low Speed Wind Tunnel Testing*, Department of Aeronautics and Astronautcs, Naval Postgraduate School, Monterey, Ca., August 1989.

12. Kersh, J. M., Jr., *Lift Enhancement Using Close-Coupled Canard/Wing Vortex Interaction*, Master's Thesis, Naval Postgraduate School, Monterey, Ca., December 1990.

13. Schmidt, D. C., *Lift Enhancement Using a Close-Coupled Oscillating Canard*, Master's Thesis, Naval Postgraduate School, Monterey, Ca., September 1992.

14. Stuart, T. D., *Experimental Study of the Effect of Helical Grooves on an Infinite Cylinder*, Engineer's Degree, Naval Postgraduate School, Monterey, Ca., December 1992.

APPENDIX A. BALANCE CALIBRATION

The external strain-gage balance used was built to measure axial and normal forces and pitching moment in the NPS low speed wind tunnel. The balance was designed with two pairs of orthogonal strain-gage bridges mounted on flexure links with 26.5 inches of vertical separation as shown in Figure A1. Each external strain-gage bridge had four active legs for automatic temperature compensation. The calibration procedure began by attaching the calibration rig to the balance. Figure A2 shows the calibration rig in place with the pulley translating vertical forces to horizontal forces from suspended weights. The amplifier gain was set at 1000 and the MC-MIO-16L-9 board gain set to one. Prior to adding weights, the amplifiers and signal conditioners were zeroed. The span control on the signal conditioner was set to 10 VDC. With the amplifier input shorted, the output and input was zeroed at amplifier gains of 1 and 1000. The shorting plugs were removed, channels zeroed, and the acquisition program started. The turntable was rotated to both 0 and 90 degrees and weights were suspended from the rig at two different heights. Measurements of E_{aa}, E_{ba}, E_{an}, and E_{bn} were recorded as the weights were added and removed.

Four calibration runs were conducted, two in the normal direction and two in the axial direction, with the cable at

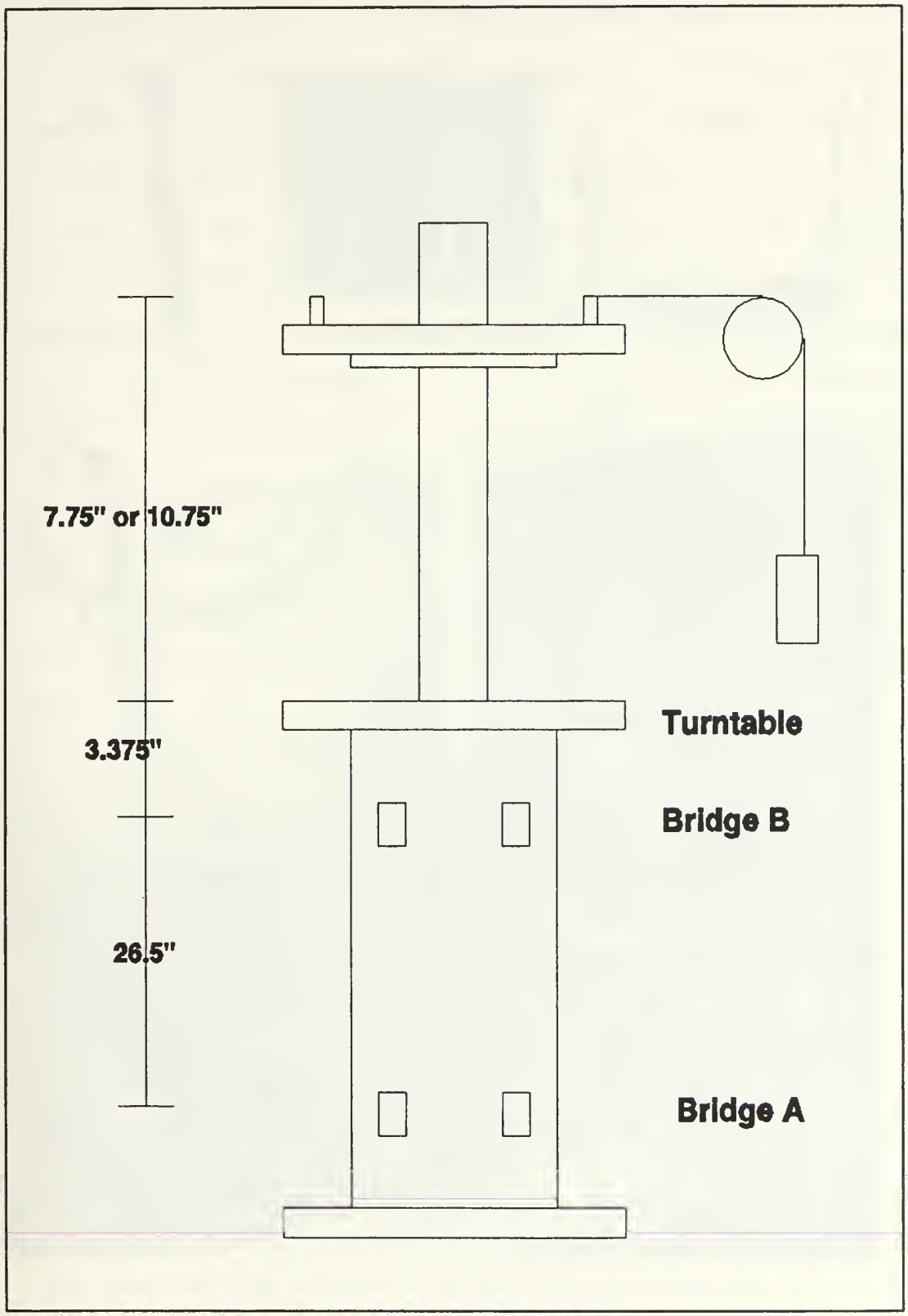

Figure A1. Strain Gage Balance Diagram

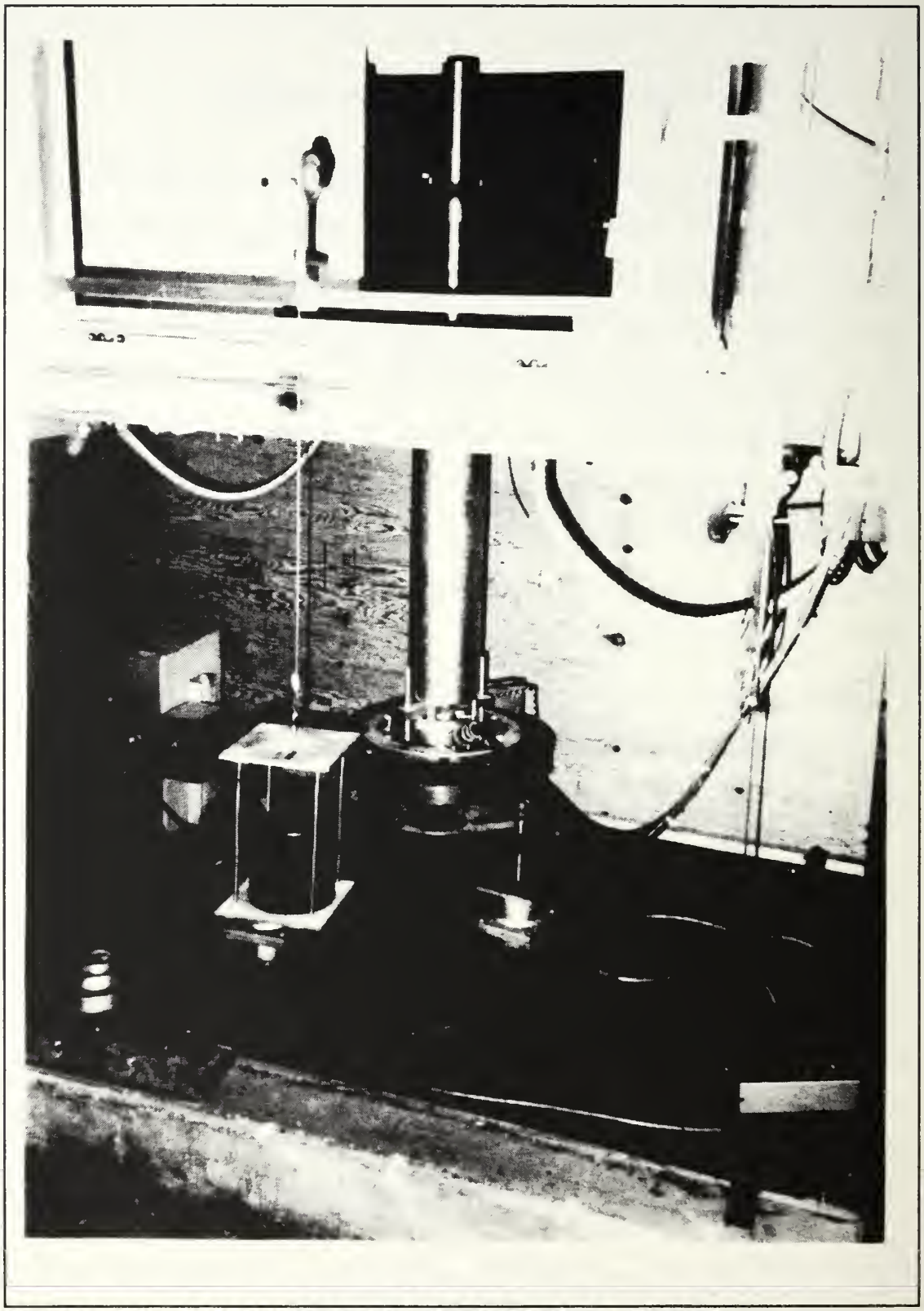

Figure A2. Calibration Rig Installed in Tunnel

10.75 and 7.75 inches of height as referenced to the tunnel floor. Normal forces were perpendicular to the tunnel walls. Note that the balance was rotated to 90 degrees when the wing/strake/body was defined to be at 0 degrees AOA. This was to account for the turntable rotational limits of -18 and +200 degrees of revolution. Figure A3 illustrates the sign convention used. The data were analyzed and plots of balance voltage versus calibration load were made. The plots are Figures A4, A5, A6, and A7. Linear regression was conducted to determine $d\Delta E/dload$ for each of the 16 lines. The figures show the linearity expected from elastic loading, and the small interaction between channel bridges. Figures A6 and A7 reveal reduced sensitivity in the E_{ba} channel. This was due to two legs on the bridge circuit being replaced by a constant-reference resistance gage during previous research [Ref. 14]. Balance nomenclature is as follows:

Ean Voltage at the lower normal force bridge
Eaa Voltage at the lower axial force bridge
Ebn Voltage at the upper normal force bridge
Eba Voltage at the upper axial force bridge
(a - b) Height above turntable of 1st cable attachment pt.
(a'- b) Height above turntable of 2nd cable attachment pt.

The goal of the calibration was the calculation of the 4x4 calibration matrix, [K]. When [K] is post-multiplied by

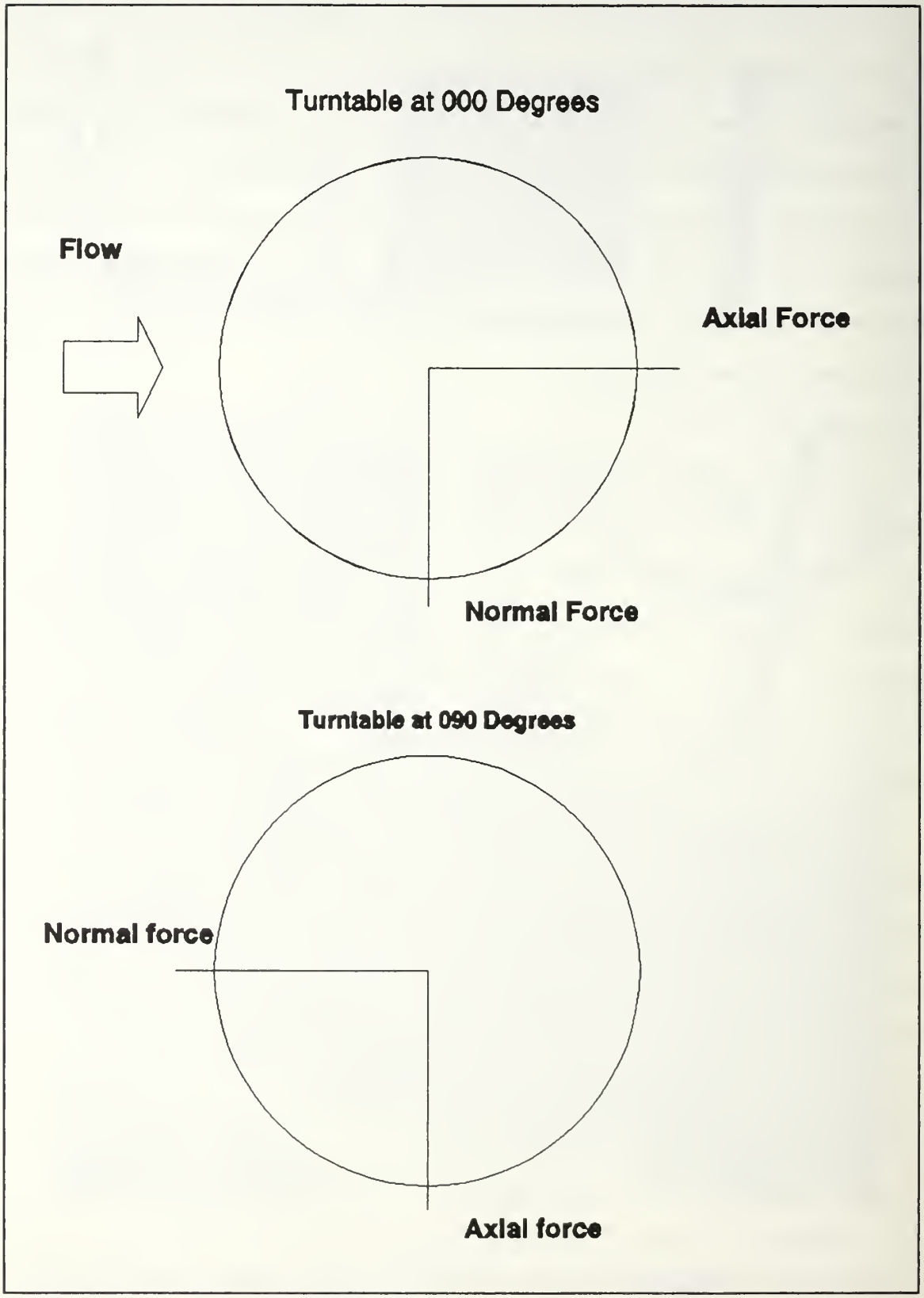

Figure A3. Sign Convention

output voltages, forces and moments are produced. Equation A1 was the basic equation used in determining the axial and normal forces and moments.

$$[K]\left[\frac{d\Delta E}{dLOAD}\right] = \begin{bmatrix} AXIALFORCE \\ AXIALMOMENT \\ NORMALFORCE \\ NORMALMOMENT \end{bmatrix} \qquad \textbf{(A1)}$$

Expanding (A1) into 4 x4 matrices yields equation A2.

$$\begin{bmatrix} K_{11} & K_{12} & K_{13} & K_{14} \\ K_{21} & K_{22} & K_{23} & K_{24} \\ K_{31} & K_{32} & K_{33} & K_{34} \\ K_{41} & K_{42} & K_{43} & K_{44} \end{bmatrix} \begin{bmatrix} \frac{d\Delta Eaa}{dA} & \frac{d\Delta E'aa}{dA} & \frac{d\Delta Eaa}{dN} & \frac{d\Delta E'aa}{dN} \\ \frac{d\Delta Eba}{dA} & \frac{d\Delta E'ba}{dA} & \frac{d\Delta Eba}{dN} & \frac{d\Delta E'ba}{dN} \\ \frac{d\Delta Ean}{dA} & \frac{d\Delta E'an}{dA} & \frac{d\Delta Ean}{dN} & \frac{d\Delta E'an}{dN} \\ \frac{d\Delta Ebn}{dA} & \frac{d\Delta E'bn}{dA} & \frac{d\Delta Ebn}{dN} & \frac{d\Delta E'ba}{dN} \end{bmatrix}$$

$$= \begin{bmatrix} 1 & 1 & 0 & 0 \\ (a\text{-}b) & (a'\text{-}b) & 0 & 0 \\ 0 & 0 & 1 & 1 \\ 0 & 0 & (a\text{-}b) & (a'\text{-}b) \end{bmatrix} \qquad \textbf{(A2)}$$

The right hand side of equation (A2) was known. The dΔE/dload matrix came from the linear regressions previously determined. The [K] matrix was found by inverting the dΔE/dLOAD matrix and post multiplying. [Ref. 9, 13, 14]

$$[K] = \begin{bmatrix} 0.0084 & -0.0046 & 0.0006 & -0.0007 \\ -0.0343 & 0.2190 & 0.0020 & -0.0049 \\ -0.0007 & 0.0016 & 0.0095 & -0.0047 \\ 0.0087 & -0.0297 & -0.0464 & 0.1616 \end{bmatrix} \qquad \textbf{(A3)}$$

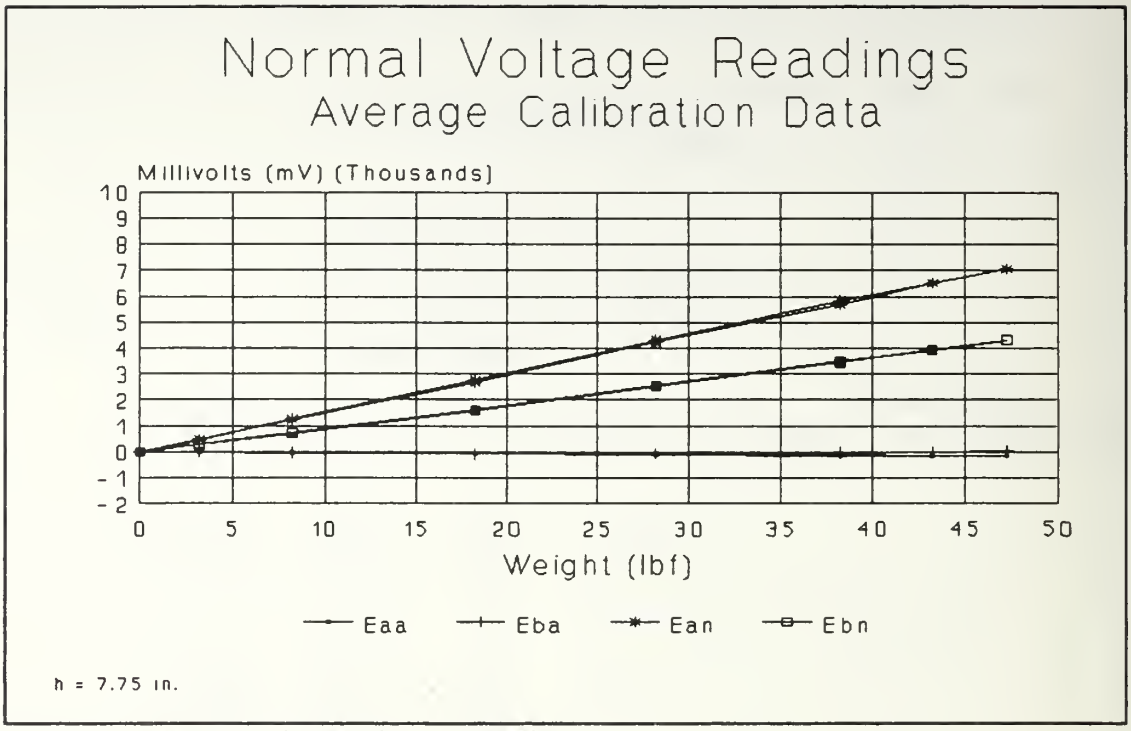

Figure A4. Calibration Loading

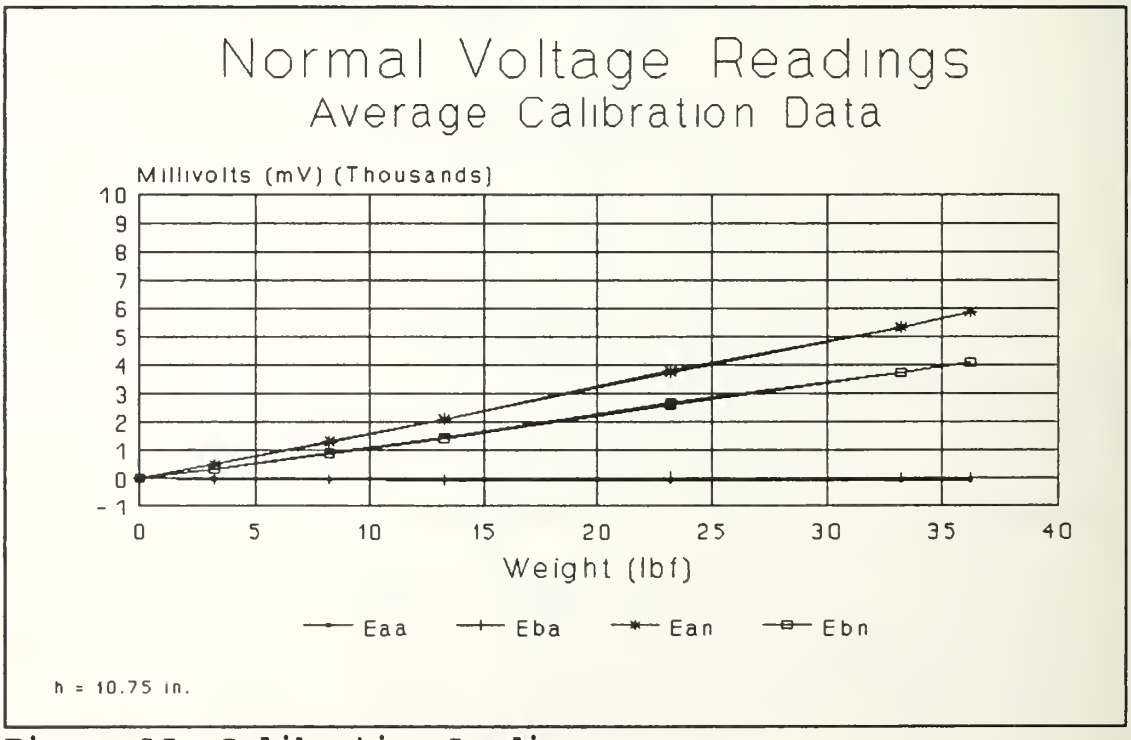

Figure A5. Calibration Loading

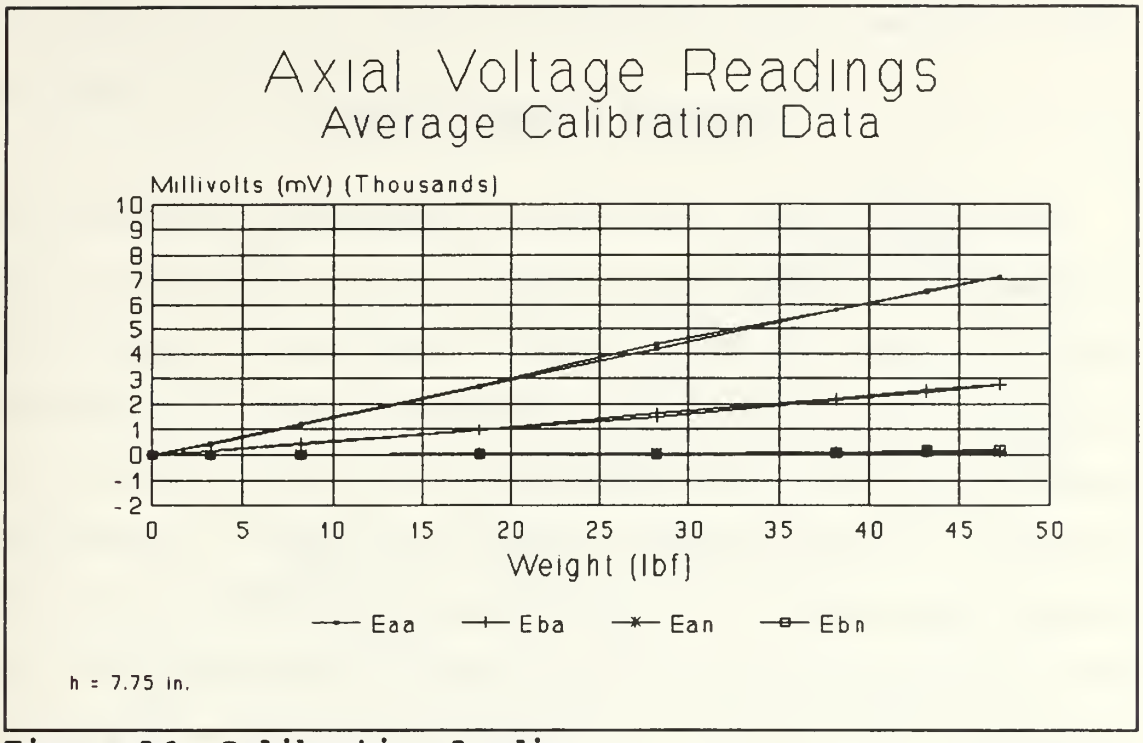

Figure A6. Calibration Loading

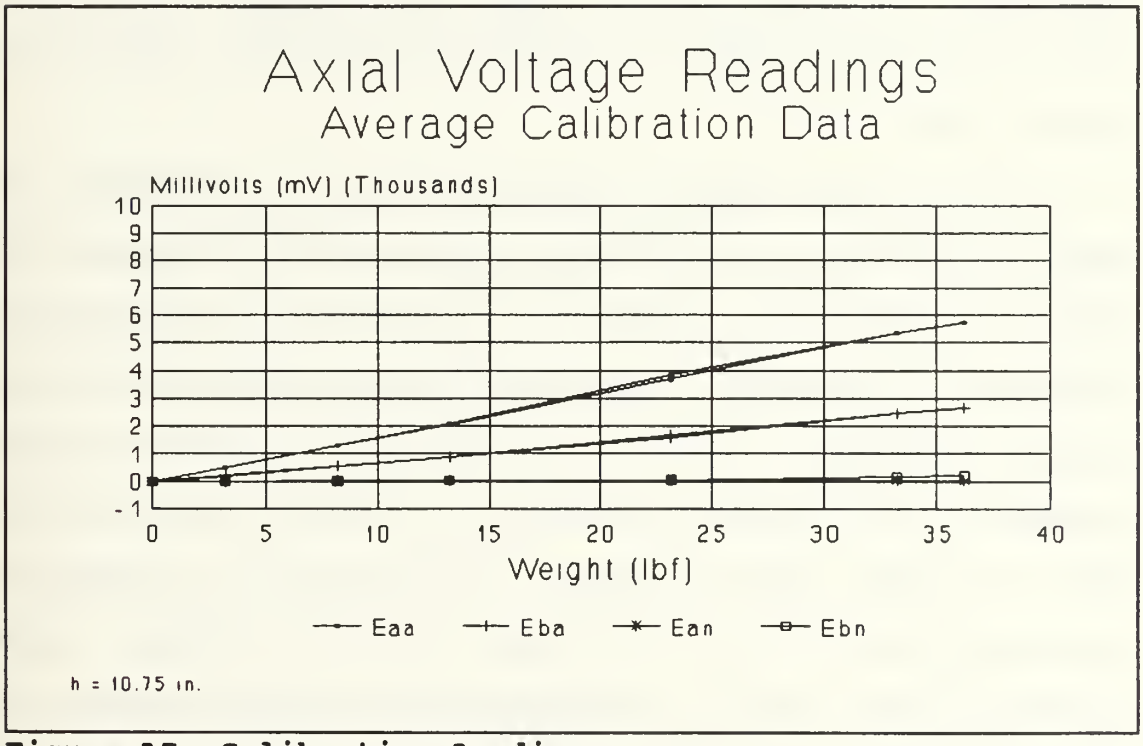

Figure A7. Calibration Loading

APPENDIX B. MODEL DESIGN

The wing/strake for the model, designed by LT Jim Willson, was generally based on the design of the wing/strake model used in a numerical study by Kern. The Kern design provided predicted lift and drag performance and vortex flow patterns for the planform. The predicted data of the wing only will allow for follow-on study of the interaction of the forebody vortex, generated by the wind-tunnel model fuselage, with the strake and wing vortices. The vortex flow patterns will be of tremendous use in any flow visualization follow-on research conducted. However, there were some distinct differences between the Kern design and the Willson design used in this study. [Ref. 9,10]

The Kern study used a flat plate with beveled edges. That approach was optimal for vortex generation and numerical grid generation; however, it did not represent the modern tactical fighter wing of today. The modern fighter does not have flat plates for wings. Willson patterned his wing after current fighters. He chose a NACA-64A008 airfoil section for the wing. The eight percent thickness was chosen as representative of the thickness found on current fighter aircraft. The strake was designed with a sharp leading edge to facilitate vortex generation. It is wedge shaped and has a wedge angle of 18 degrees. The wing/strake geometric

characteristics are shown in Figure B1 and listed in Table B1.[Ref. 9, 10]

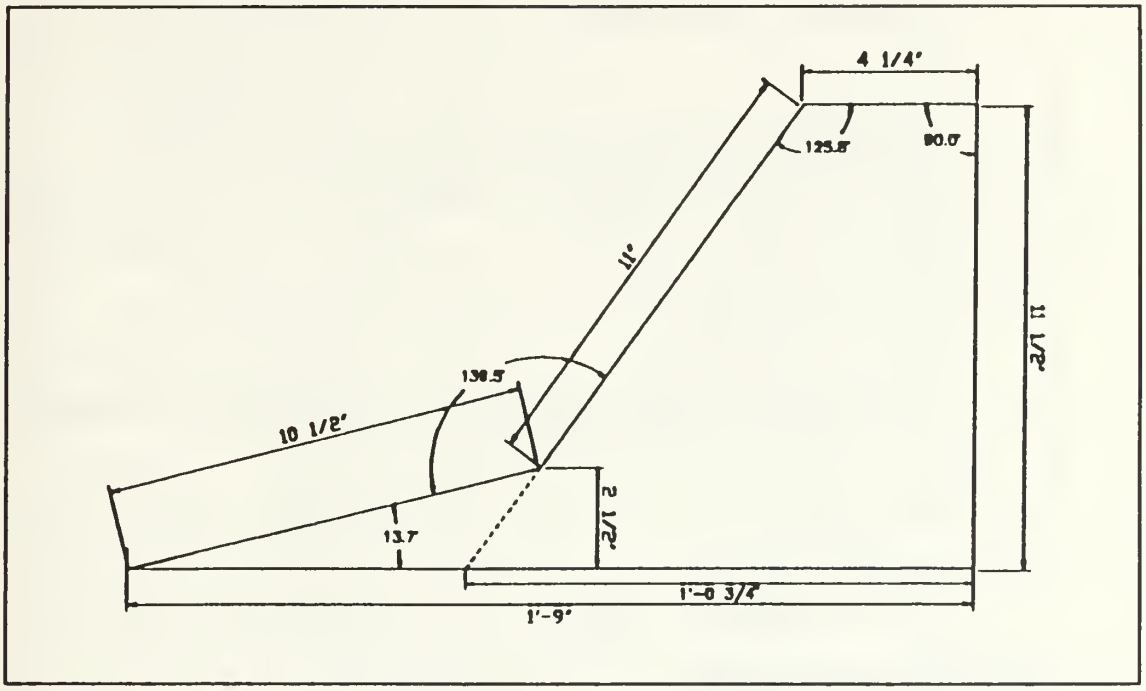

Figure B1. Wing/Strake Geometric Characteristics [Ref. 9]

The Kern study did not have a fuselage section. The lack of a fuselage prevented the examination of forebody vortices interaction with wing/strake vortices. The model for this study and that done by Willson had a fuselage with an ogive forebody. The fuselage for this study is identical to the fuselage used by Kersh, Schmidt, and Willson. The wing was designed to be removable to facilitate other research. [Ref. 9, 12, 13]

The wing/strake was positioned on the fuselage side as shown in Figure B2 (the normal force vector is towards the bottom of the figure). Figure B3 shows the locations of the

TABLE B1.

Airfoil Section	NACA 64A008
Wing Area (semi-span)	
Projected[1]	0.969 ft^2
Exposed	0.679 ft^2
With Strake (exposed)	0.750 ft^2
Chord	
Root (exposed)	12.75 in
Root (centerline)	15.00 in
With Strake (exposed)	21.00 in
Aspect Ratio (w/o strake)	1.51
Taper Ratio	0.283
Sweepback Angle	35.8°
Mean Aerodynamic Chord	10.63 in
Incidence Angle	0°
Dihedral Angle	0°
Twist angle	0°

blowing ports. Port 3 was used by Willson and Howard, it was not used in this study. The inclination angles, as shown in Figure B3, were measured with the reference axis parallel to the strake-fuselage junction. A positive inclination angle would be toward the bottom of Figure B3. The blowing tubes were secured in the blowing ports via set screws in an aluminum bracket. The tube angle was the amount of bend, or sweep, in the tube.

1 Wing Reference Area

Figures B4 through B6 are photos of the combined wing model and blowing tube as installed in the tunnel.

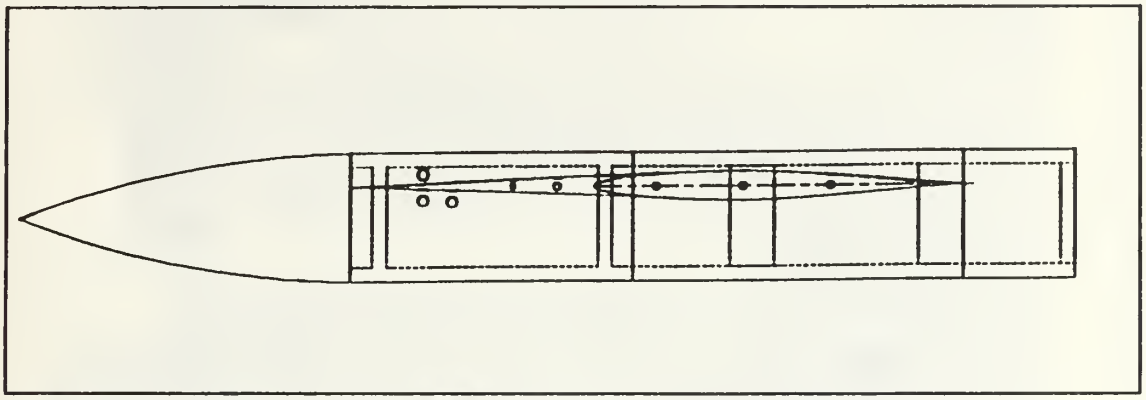

Figure B2. Top View of Wing/Strake Model [Ref. 9]

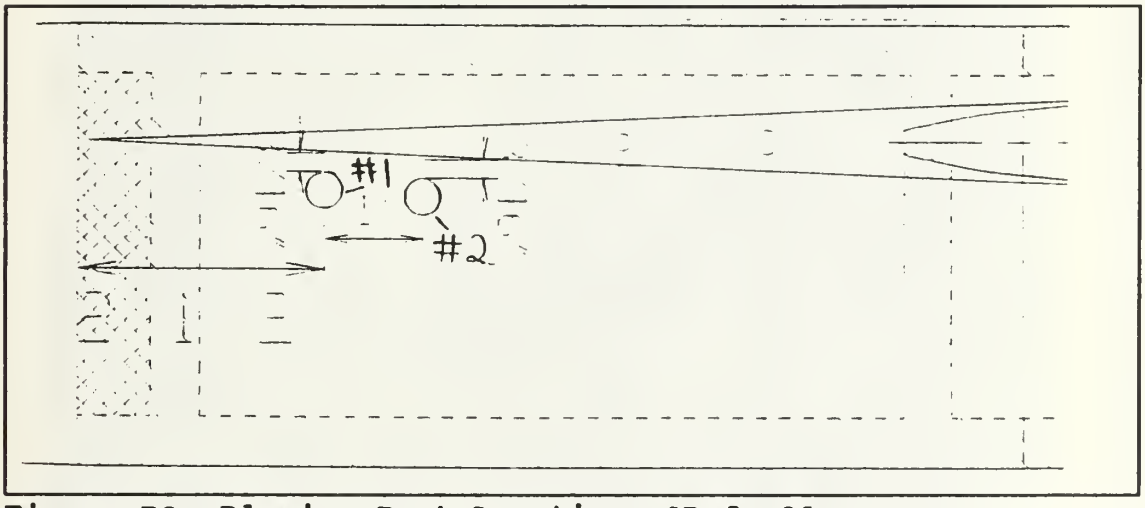

Figure B3. Blowing Port Locations [Ref. 9]

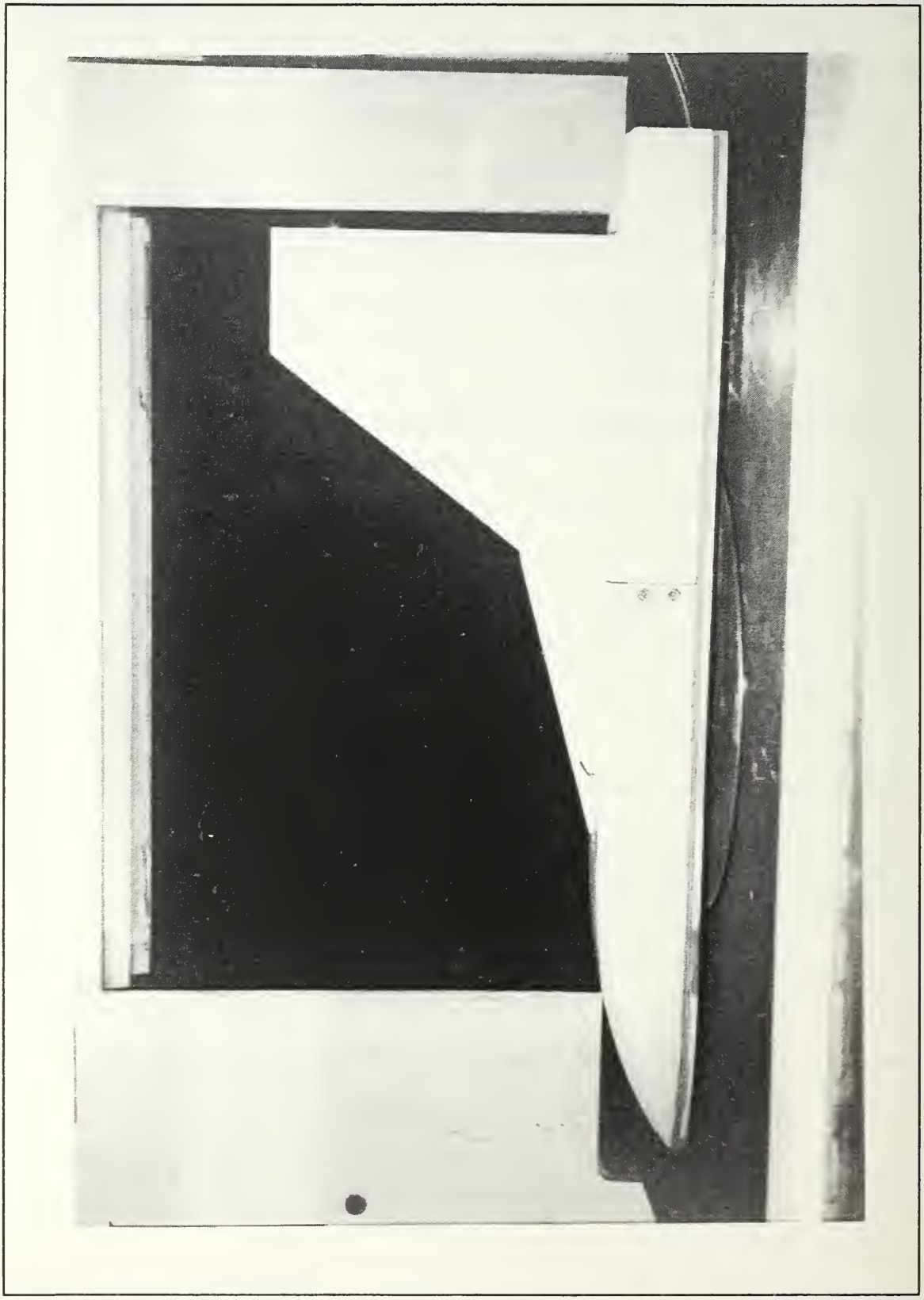

Figure B4. Side View of Model in Tunnel

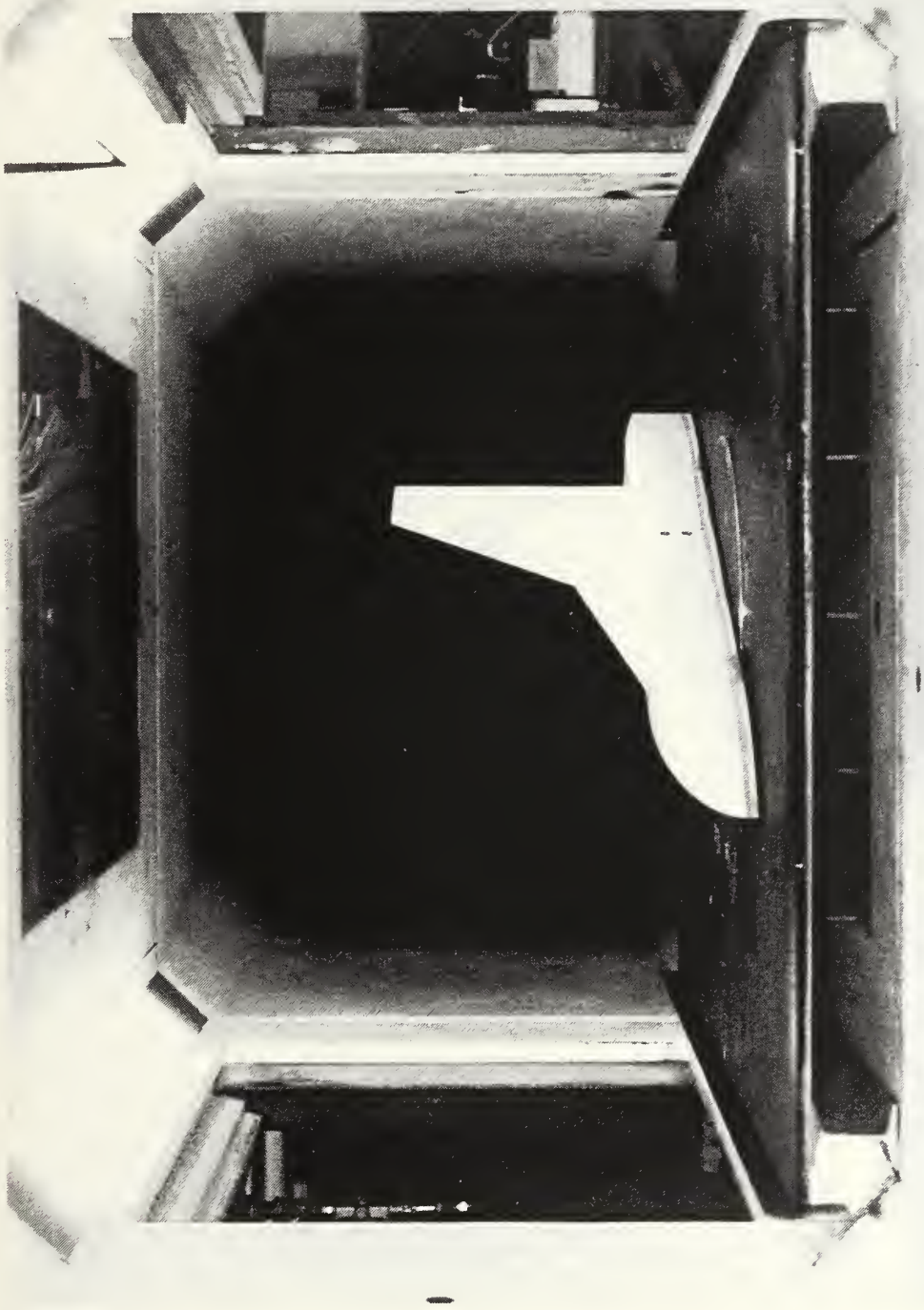

Figure B5. Front View of Model in Tunnel

Figure B6. Close-up of Blowing Tube on Model

APPENDIX C. ADDITIONAL FIGURES

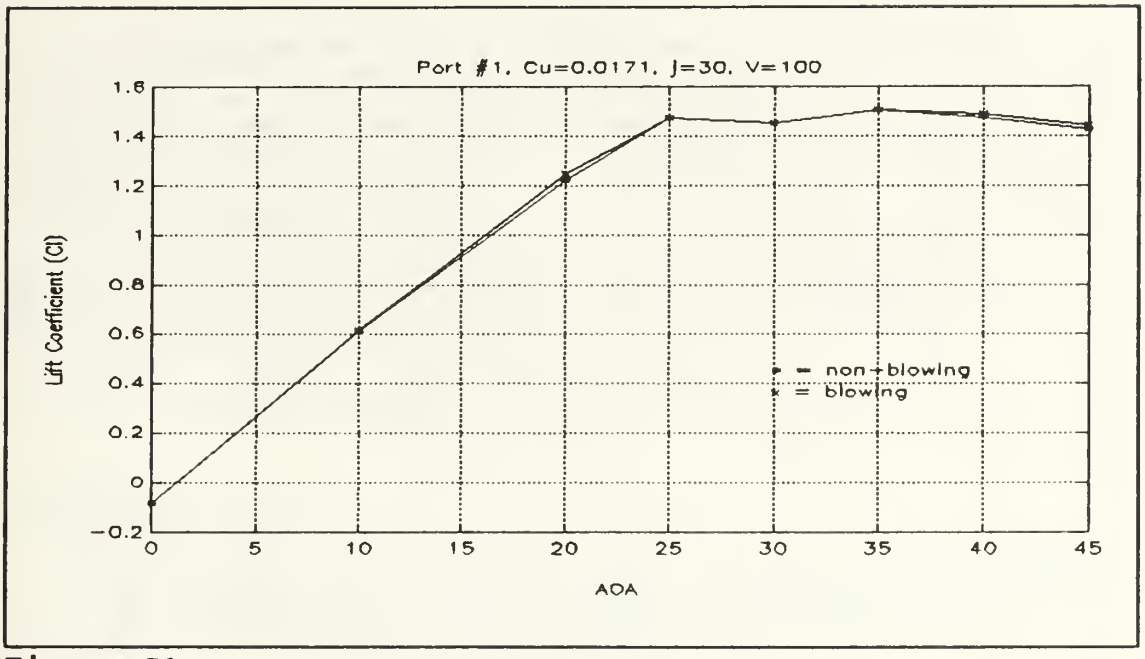

Figure C1.

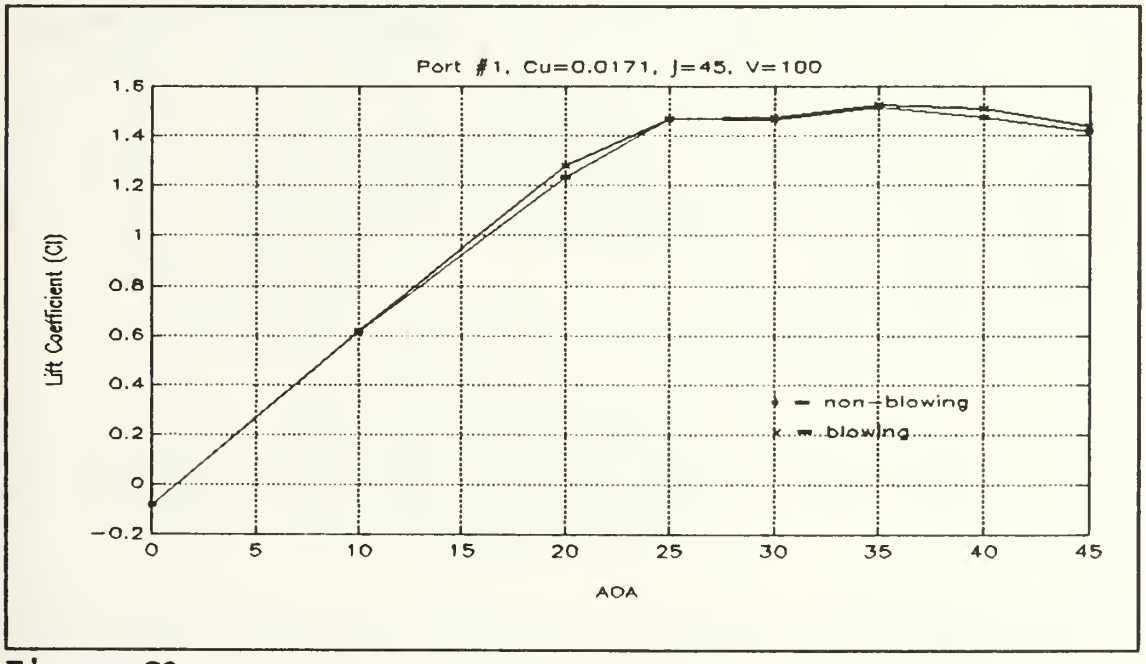

Figure C2.

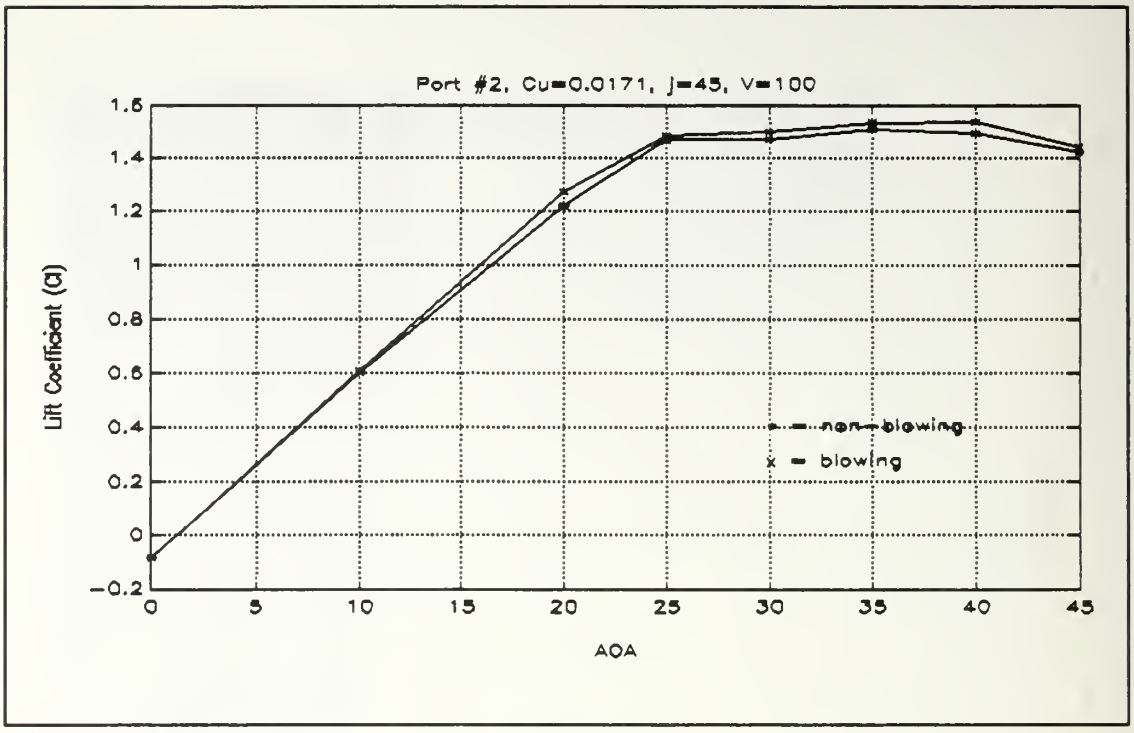

Figure C4.

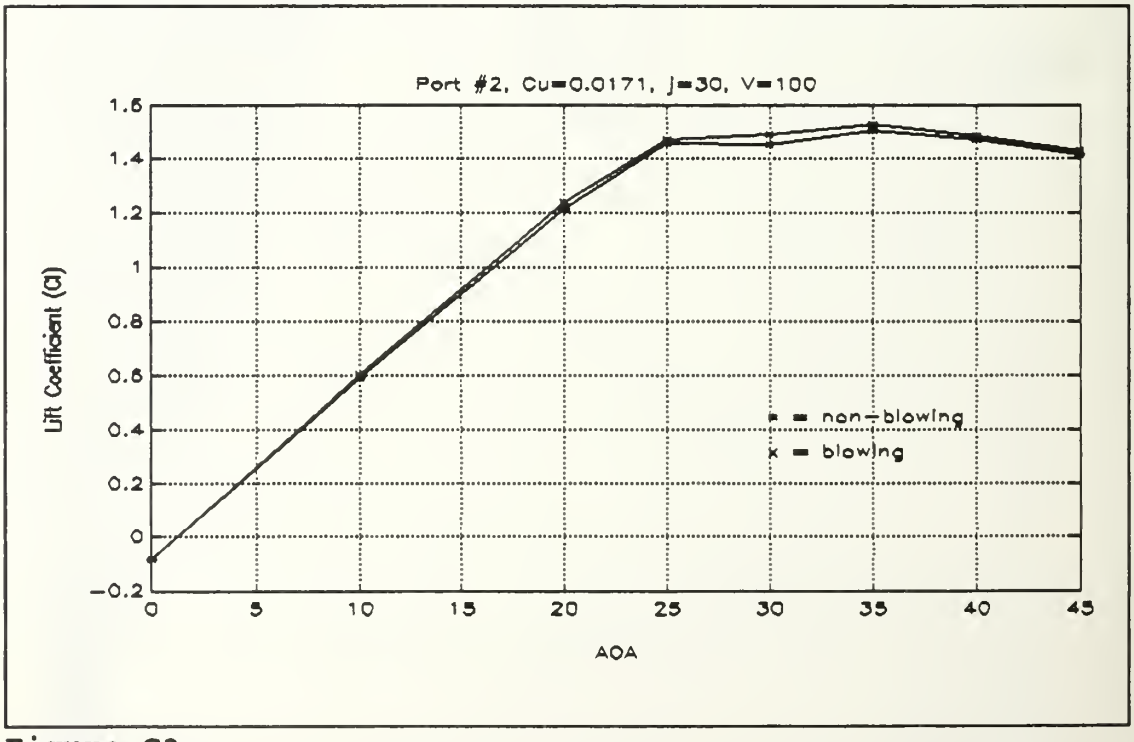

Figure C3.

APPENDIX D. DATA ACQUISITION PROGRAM

```
'       This program was written and compiled using LabWindows and
'  QuickBasic 4.5.  (used "bc /o multi" to compile)  It's purpose
'  is to read and convert voltages from four channels connected to
'  the strain gauges on the Acedemic wind tunnel.  The voltages are
'  converted to normal and axial forces and moments with respect to
'  the balance.  It was written and modified by LT Tom D. Stuart and
'  LT Dean C. Schmidt, 20 June 92.
'       Modified, 14 AUG 92, by LT James G. Willson to conform to data
'  parameters for pneumatic blowing tests.  Since runs are conducted in
'  parallel during blowing tests, different color screens are used to
'  verify to the operator what phase of the program he/she is in.  The
'  following is the color scheme:
'                Green:  Test Parameters
'                Blue:   Blowing OFF
'                Red:    Blowing ON


'  Variables explained

'       eaa = Strain gauge voltage at point A in Axial direction.
'       eba = Strain gauge voltage at point B in Axial direction.
'       ean = Strain gauge voltage at point A in Normal direction.
'       ebn = Strain gauge voltage at point B in Normal direction.

'       AX  = Axial force
'       Max = Axial moment
'       NORM = Normal force
'       Mnorm = Normal moment

'       alpha = Angle of Attack of the model
'       tube = Blowing tube position
'       blow = Blowing Coefficient (Cmhu)
'       Jangle = Jet angle of the tube
'       Iangle = Angle of incidence of the tube
'       LIFT = Lift force
'       DRAG = Drag force

'*****************************************************************************

REM     $INCLUDE: 'C:\LW\INCLUDE\LWSYSTEM.INC'
REM     $INCLUDE: 'C:\LW\INCLUDE\GPIB.INC'
REM     $INCLUDE: 'C:\LW\INCLUDE\FORMATIO.INC'
REM     $INCLUDE: 'C:\LW\INCLUDE\GRAPHICS.INC'
REM     $INCLUDE: 'C:\LW\INCLUDE\ANALYSIS.INC'
REM     $INCLUDE: 'C:\LW\INCLUDE\DATAACQ.INC'
REM     $INCLUDE: 'C:\LW\INCLUDE\RS232.INC'

DIM K#(4,4)
DIM ean.array#(1000),eaa.array#(1000),ebn.array#(1000),eba.array#(1000)
COMMON SHARED ean.array#(),eaa.array#(),ebn.array#(),eba.array#()

DECLARE SUB volt (ean#,eaa#,ebn#,eba#,alpha!)
DECLARE SUB aero (AX#,NORM#,LIFT#,DRAG#,alpha!)
DECLARE SUB forces (K#(),eaa#,eba#,ean#,ebn#,AX#,Max#,NORM#,Mnorm#,alpha!)
```

```
SCREEN 9, 0
COLOR 15, 1

ANS2$ = "N"
C$="N"

'  Set non-blowing tares to zero
eaa0# = 0
eba0# = 0
ean0# = 0
ebn0# = 0

'  Set blowing tares to zero
eaa0b# = 0
eba0b# = 0
ean0b# = 0
ebn0b# = 0

'*************************************************************************

' CALIBRATION MATRIX INPUT (See Dean Schmidt's thesis for explaination)

DATA  0.0084,     -0.0046,     0.0006,    -0.0007
DATA -0.0343,      0.2190,     0.0020,    -0.0049
DATA -0.0007,      0.0016,     0.0095,    -0.0047
DATA  0.0087,     -0.0297,    -0.0464,     0.1616

FOR L% = 1 TO 4: FOR M% = 1 TO 4
READ K#(L%,M%) : NEXT M%
NEXT L%

'*************************************************************************

CLS: LOCATE 05, 20: PRINT "Type the last six characters of"
LOCATE 06, 20: INPUT "your output files:"; DFILE$
VOL$ = "C:\LW\INSTR\CRAIG\NV" + DFILE$ + ".DAT"
OPEN VOL$ FOR APPEND AS #1
BVOL$ = "C:\LW\INSTR\CRAIG\BV" + DFILE$ + ".DAT"
OPEN BVOL$ FOR APPEND AS #2
FM$ = "C:\LW\INSTR\CRAIG\NF" + DFILE$ + ".DAT"
OPEN FM$ FOR APPEND AS #3
BM$ = "C:\LW\INSTR\CRAIG\BF" + DFILE$ + ".DAT"
OPEN BM$ FOR APPEND AS #4
COLOR 15, 2
LOCATE 10, 10
PRINT "DATA FILES ARE:"
PRINT "                "; VOL$
PRINT "                "; BVOL$
PRINT "                "; FM$
PRINT "                "; BM$
INPUT "COPY THEM ONTO CHECKLIST."; ZZ$

'  See Lt. Willson's thesis for tube position numbering.
CLS: LOCATE 10, 20: INPUT "Blowing tube position? (1,2,3)"; Tube%
LOCATE 15, 20: INPUT "Input tube jet angle (deg)"; Jangle!
LOCATE 20, 20: INPUT "Input tube incidence angle (deg)"; Iangle!

500
COLOR 15, 2
CLS: LOCATE 10, 20: PRINT "Input the Test AOA"
LOCATE 11, 20: INPUT "from turntable markings (deg.)"; alpha!
alpha! = 90 - alpha!
```

```
LOCATE 20, 20: INPUT "Input blowing coefficient (Cu)"; blow!

'  Prevent asking for tare calculation a second time.  ANS$ is defined
'  as "N" at the begining of the program and must be <> "N" in order
'  to loop back to 500.

IF ANS2$ <> "N" THEN
   COLOR 15, 1
   GOTO 600
END IF

COLOR 15, 1
CLS: LOCATE 5, 20: INPUT "Is this a tare (zero load) reading? (Y/N)"; A$

IF A$ = "Y" THEN
   CALL tare (ean0#,eaa0#,ebn0#,eba0#,alpha!,tube%,0.0,Jangle!,Iangle!)
700
   LOCATE 15, 20:  INPUT "Are blowing tares to be taken? (Y/N)"; C$

   IF C$ = "Y" THEN
      COLOR 15, 4
                              C    A    L    L           t    a    r    e
(ean0b#,eaa0b#,ebn0b#,eba0b#,alpha!,tube%,blow!,Jangle!,Iangle!)
      COLOR 15, 1
   ELSEIF C$ = "N" THEN
      LOCATE 17, 10: PRINT "Setting blowing tare in program equal to
non-blowing tare."
      eaa0b# = eaa0#
      eba0b# = eba0#
      ean0b# = ean0#
      ebn0b# = ebn0#
   ELSE
      GOTO 700
   END IF
   C$ = "N"

ELSE LOCATE 15, 20: PRINT "Data will not be accurate!!!"
END IF

600
LOCATE 22,20: INPUT "Ready to take readings? (Y/N)"; B$

LOCATE 23,20: INPUT "HOW MANY SAMPLES?"; NSAMP%

IF B$ = "y" THEN
   CLS: LOCATE 15,20: PRINT "TURN ON CAPS LOCK"
   GOTO 600
END IF

IF B$ <> "Y" THEN GOTO 5000

LOCATE 24, 20: INPUT "Is this with blowing or not? (B/N)"; BN$

FOR NN% = 1 TO NSAMP%

IF B$ = "Y" THEN CALL volt (ean#,eaa#,ebn#,eba#,alpha!)

' Correcting for zero load values.

IF BN$ = "N" THEN
  COLOR 15, 1
  eaa# = eaa# - eaa0#
```

```
  eba# = eba# - eba0#
  ean# = ean# - ean0#
  ebn# = ebn# - ebn0#
ELSEIF BN$ = "B" THEN
  COLOR 15, 4
  eaa# = eaa# - eaa0b#
  eba# = eba# - eba0b#
  ean# = ean# - ean0b#
  ebn# = ebn# - ebn0b#
ELSE
  CLS: COLOR 12, 0
  LOCATE 15, 10: PRINT "BAD ANSWER TO BLOWING QUESTION.  CHECK CAPLOCK.
NODATA RECOERDED!!"
  GOTO 600
END IF

CALL forces (K#(),eaa#,eba#,ean#,ebn#,AX#,Max#,NORM#,Mnorm#,alpha!)

CALL aero (AX#,NORM#,LIFT#,DRAG#,alpha!)

PRINT " "
PRINT "          AOA           EAA (mV)        EBA (mV)        EAN (mV)
EBN (mV)"
PRINT "     **********       **********      **********      **********
**********"

PRINT USING "    ####.######";  alpha!; eaa#; eba#; ean#; ebn#

PRINT " "
PRINT "     AXIAL (lb)      MOMax (ft-lb)  NORMAL (lb)    MOMnorm(ft-lb)"
PRINT "    ***********     *************  ***********    ***************"

PRINT USING "    ####.######";  AX#; Max#; NORM#; Mnorm#

PRINT " "
PRINT "                                          Blowing          Jet
Inclination"
PRINT "      Lift (lb)       Drag (lb)        Coeff        Angle (deg)
Angle (deg)"
PRINT "    ***********     ***********     ***********     ***********
***********"

PRINT USING "    ####.######"; LIFT#; DRAG#;blow!;Jangle!;Iangle

IF BN$ = "B" THEN
      P R I N T    # 2 ,    U S I N G    " # # # # # . # # # # # # " ;
alpha!;blow!;Jangle!;Iangle!;eaa#;eba#;ean#;ebn#
           P   R   I   N   T         #   4   ,         U   S   I   N   G
"####.#####";alpha!;blow!;Jangle!;Iangle!;AX#;NORM#;LIFT#; DRAG#
ELSE
      P R I N T    # 1 ,    U S I N G    " # # # # # . # # # # # # " ;
alpha!;blow!;Jangle!;Iangle!;eaa#;eba#;ean#;ebn#
           P   R   I   N   T         #   3   ,         U   S   I   N   G
"####.#####";alpha!;blow!;Jangle!;Iangle!;AX#;NORM#;LIFT#; DRAG#
END IF

NEXT NN%

LOCATE 21, 20: INPUT "Do you want another reading?  (Y/N)"; ANS$
IF ANS$ = "Y" THEN
   LOCATE 22, 20: INPUT "New parameters?  (Y/N)"; ANS2$
   IF ANS2$ = "N" THEN GOTO 600
```

```
   IF ANS2$ <> "N" THEN GOTO 500
END IF

5000 CLOSE #1
CLOSE #2
CLOSE #3
CLOSE #4

END

'************************************************************************
'************************************************************************
SUB volt (ean#,eaa#,ebn#,eba#,alpha!)
'************************************************************************
'
' S/R to read Channel 0,2,4,6 on MIO-16L-9 for Analog Voltage
'
'************************************************************************

'  Setting Board code for MIO-16L-9

board.code%=0

'************************************************************************


err1.num% = Init.DA.Brds(1, board.code%)

err2.num% = AI.Setup(1, 0, 1)
err3.num% = AI.Setup(1, 2, 1)
err4.num% = AI.Setup(1, 4, 1)
err5.num% = AI.Setup(1, 6, 1)

' Configure and set clock to 1MHZ

err6.num% = CTR.Clock (1, 1, 1, 1)
err7.num% = CTR.Config (1, 1, 0, 0, 0, 0)

LWtotal! = 0

FOR i% = 1 TO 1000

err8.num% = CTR.EvCount (1, 1, 1, 0)

' CH 0 = Eaa
        err9.num% = AI.Read(1, 0, 1, value0%)
        er10.num% = AI.Scale(1, 1, value0%, eaa.array#(i%))

' CH 2 = Eba
        er11.num% = AI.Read(1, 2, 1, value2%)
        er12.num% = AI.Scale(1, 1, value2%, eba.array#(i%))

' CH 4 = Ean
        er13.num% = AI.Read(1, 4, 1, value4%)
        er14.num% = AI.Scale(1, 1, value4%, ean.array#(i%))

' CH 6 = Ebn
        er15.num% = AI.Read(1, 6, 1, value6%)
        er16.num% = AI.Scale(1, 1, value6%, ebn.array#(i%))

er17.num% = CTR.EvRead (1, 1, overflo%, tcount%)
```

```
LWtotal! = LWtotal! + tcount%

NEXT i%

CLS:LOCATE 5,15:PRINT "Total Time is " LWtotal!*1E-6" seconds."

CALL Mean (eaa.array#(), 1000, eaa#)
CALL Mean (eba.array#(), 1000, eba#)
CALL Mean (ean.array#(), 1000, ean#)
CALL Mean (ebn.array#(), 1000, ebn#)


'************************************************************************

' This multiplication (*1000) will make the voltages in mV

eaa#=eaa#*1000
eba#=eba#*1000
ean#=ean#*1000
ebn#=ebn#*1000

END SUB


'************************************************************************
'************************************************************************


SUB forces (K#(),eaa#,eba#,ean#,ebn#,AX#,Max#,NORM#,Mnorm#,alpha!)

' FORCES AND MOMENTS CALCULATIONS (See thesis for explaination)

AX# = K#(1,1)*eaa# + K#(1,2)*eba# + K#(1,3)*ean# + K#(1,4)*ebn#
Max# = K#(2,1)*eaa# + K#(2,2)*eba# + K#(2,3)*ean# + K#(2,4)*ebn#
NORM# = K#(3,1)*eaa# + K#(3,2)*eba# + K#(3,3)*ean# + K#(3,4)*ebn#
Mnorm# = K#(4,1)*eaa# + K#(4,2)*eba# + K#(4,3)*ean# + K#(4,4)*ebn#

END SUB

'************************************************************************
'************************************************************************

SUB aero (AX#,NORM#,LIFT#,DRAG#,alpha!)

'************************************************************************

PI# = 3.14159265359

' Transformed due to balance offset of 90 degrees.

LIFT# = AX# * COS(PI#/180*alpha!) + NORM# * SIN(PI#/180*alpha!)

DRAG# = AX# * SIN(PI#/180*alpha!) - NORM# * COS(PI#/180*alpha!)

END SUB

'************************************************************************
'************************************************************************
SUB tare (ean#,eaa#,ebn#,eba#,alpha!,tube%,blow!,Jangle!,Iangle!)
'************************************************************************
'
' S/R to read Channel 0,2,4,6 on MIO-16L-9 for Analog Voltage
```

```
'
'*************************************************************************

'  Setting Board code for MIO-16L-9

board.code%=0

'*************************************************************************

CLS: LOCATE 5, 20: INPUT "Ready to take tare readings? (Y/N)"; T$

IF T$ <> "Y" THEN RETURN

err1.num% = Init.DA.Brds(1, board.code%)

err2.num% = AI.Setup(1, 0, 1)
err3.num% = AI.Setup(1, 2, 1)
err4.num% = AI.Setup(1, 4, 1)
err5.num% = AI.Setup(1, 6, 1)

' Configure and set clock to 1MHZ

err6.num% = CTR.Clock (1, 1, 1, 1)
err7.num% = CTR.Config (1, 1, 0, 0, 0, 0)

LWtotal! = 0

FOR i% = 1 TO 1000

err8.num% = CTR.EvCount (1, 1, 1, 0)

' CH 0 = Eaa
        err9.num% = AI.Read(1, 0, 1, value0%)
        er10.num% = AI.Scale(1, 1, value0%, eaa.array#(i%))

' CH 2 = Eba
        er11.num% = AI.Read(1, 2, 1, value2%)
        er12.num% = AI.Scale(1, 1, value2%, eba.array#(i%))

' CH 4 = Ean
        er13.num% = AI.Read(1, 4, 1, value4%)
        er14.num% = AI.Scale(1, 1, value4%, ean.array#(i%))

' CH 6 = Ebn
        er15.num% = AI.Read(1, 6, 1, value6%)
        er16.num% = AI.Scale(1, 1, value6%, ebn.array#(i%))

er17.num% = CTR.EvRead (1, 1, overflo%, tcount%)

LWtotal! = LWtotal! + tcount%

NEXT i%

CLS:LOCATE 5,15:PRINT "Total Time is " LWtotal!*1E-6" seconds."

CALL Mean (eaa.array#(), 1000, eaa#)
CALL Mean (eba.array#(), 1000, eba#)
CALL Mean (ean.array#(), 1000, ean#)
CALL Mean (ebn.array#(), 1000, ebn#)

'*************************************************************************
```

```
' This multiplication (*1000) will make the voltages in mV

eaa#=eaa#*1000
eba#=eba#*1000
ean#=ean#*1000
ebn#=ebn#*1000

PRINT " "
PRINT "          AOA           EAA (mV)        EBA (mV)        EAN (mV)
EBN (mV)"
PRINT "     **********       **********      **********      **********
**********"

PRINT USING "    ####.######";  alpha!; eaa#; eba#; ean#; ebn#

IF blow! = 0.0 THEN
      P R I N T    # 1 ,    U S I N G    " # # # # # . # # # # # # " ;
alpha!;blow!;Jangle!;Iangle!;eaa#;eba#;ean#;ebn#
ELSE
      P R I N T    # 2 ,    U S I N G    " # # # # # . # # # # # # " ;
alpha!;blow!;Jangle!;Iangle!;eaa#;eba#;ean#;ebn#
END IF

END SUB
```

INITIAL DISTRIBUTION LIST

1.	Defence Technical Information Center Cameron Station Alexandria, VA 22304-6145	2
2.	Library, Code 52 Naval postgraduate School Monterey, CA 93940-5002	2
3.	Chairman Department of Aeronautics and Astronautics, Code AA Naval Postgraduate School Monterey, CA 93940-5000	1
4.	Steven B. Kern Naval Air Warfare Center, Aircraft Division, Code 6051 Warminster, PA 18974-5000	1
5.	NASA Ames Research Center Technical Library Moffett Field, CA 94035	1
6.	Prof. R. M. Howard Department of Aeronautics and Astronautics, Code AA/Ho Naval Postgraduate School Monterey, CA 93940-5000	3
7.	LT Craig J. Zgraggen, USN 12449 Jeremys Landing Ct. Jacksonville, FL 32258	2

229.544

Thesis
Z3443 Zgraggen
c.1 Lift enhancement of a wing/strake using pneumatic blowing.

Thesis
Z3443 Zgraggen
c.1 Lift enhancement of a wing/strake using pneumatic blowing.

AMERICAN BINDERY 1 10-93

DUDLEY KNOX LIBRARY
3 2768 00033210 0